Check for updates

Advances in harvesting water and energy from ubiquitous atmospheric moisture

Wanheng Lu,[a] Wei Li Ong[a] and Ghim Wei Ho [ID] *[ab]

Atmospheric moisture contains huge amounts of water and energy potential, which, benefiting from the advances of nanomaterials, hold great promise in delivering circular economies for the prevalent interwoven water and energy crises. Atmospheric water harvesting (AWH) and moisture-enabled energy generation (MEEG), emerging technologies capable of extracting water and energy from moisture are rapidly developing and advancing toward distributed and decentralized systems. In this review, sorbent-assisted AWH and moisture-enabled energy generation are reviewed in parallel, revealing the correlation between these two technologies. Sorbent-assisted AWH and MEEG are found to be inextricably linked in view of the similarities between both technologies with respect to the moisture/material interactions and basic material prerequisites. Mechanisms, innovative material and structural designs, as well as recent progress in developing devices, are critically discussed. Besides, AWH infrastructures integrated with renewable solar energy for water harvesting and other forms of energy conversion are covered, featuring sought-after energy efficiency and multifunctionality. Furthermore, future directions for water and energy harvesting from moisture are outlined, encompassing scientific research and practical applications.

10th anniversary statement

It has been a wonderful 10 years for JMCA publishing cutting edge advancements in materials research. Over the years, the work that we see in JMCA just keeps getting better and better, making it one of the top journals in the RSC family. Keeping in mind that the focus of the journal is on materials for energy and sustainability, this 10th anniversary milestone came just at the right time, highlighting the enormous amount of work that has been done in recent years to resolve several environmental issues, and reminding us to make the world a better place for the next generation and many generations beyond. JMCA is akin to a scientific melting pot, bringing together bright minds from all over the world, and sparking new ideas that constantly push the frontiers of knowledge. I am looking forward to many exciting years ahead with JMCA!

[a]Department of Electrical and Computer Engineering, National University of Singapore, 117583, Singapore

[b]Department of Materials Science and Engineering, National University of Singapore, 117575, Singapore. E-mail: elehgw@nus.edu.sg

Wanheng Lu received her PhD degree from the National University of Singapore (NUS) in 2017. She is currently a Research Fellow at the Department of Electrical & Computer Engineering of the NUS. Her research interests include nanomaterials and functional materials for energy and water generation, and multidimensional characterization of materials under multiple fields based on scanning probe microscopy (SPM) techniques.

Wei Li Ong received his B. Eng. (Hons.) and PhD degrees from the National University of Singapore in 2008 and 2012, respectively. He is currently a postdoctoral research fellow at the Department of Electrical & Computer Engineering at the National University of Singapore (NUS) in Prof. Ho Ghim Wei's group. His research interests primarily focus on nanomaterials for clean energy generation, photocatalytic water splitting, and atmospheric water harvesting.

12456 | *J. Mater. Chem. A*, 2023, **11**, 12456–12481

This journal is © The Royal Society of Chemistry 2023

1. Introduction

Many major cities across the globe are at risk of water and energy crises as the demand and consumption of water and energy are soaring due to population explosion, industrialization, urbanization, environmental pollution, and climate change.[1–4] To address these crises, many efforts have been devoted to exploring alternative water and energy solutions, like seawater desalination, wastewater treatment, photovoltaics, hydroelectricity, wind power, tidal energy, as well as geothermal energy. Nevertheless, these techniques seem unsustainable due to their inherent limitations in terms of geography, climate, energy fluctuation, and complex and costly installation.[5–11]

Atmospheric water or moisture is ubiquitously present in the air regardless of geographical and hydrologic conditions, and it plays a key role in the global hydrologic cycle since it holds tremendous amounts of water and energy within it.[12,13] The developments of new materials, particularly, nanostructured materials have seen advanced technologies that can extract water and energy out of this long-neglected resource, suggesting a promising and sustainable approach to address the water and energy crises. These technologies include atmospheric water harvesting (AWH) which refers to the direct generation of water from moisture, and moisture-enabled electricity generators, actuators, and heat batteries to yield electrical, mechanical, and thermal energy *via* the interaction between moisture and a variety of materials. Water and energy extraction from moisture has become a hotbed of research with a surge in the number of publications reviewing advances in atmospheric water and energy generation technologies.[14–26] However, most of these review papers either discuss the water and energy strategies separately or one type of energy conversion, without establishing an association between these strategies.

Water and energy are inextricably linked and intertwined. As such, energy is required for water production while water is often consumed for energy generation. Increasing energy efficiency can lessen the pressure on water resources, and *vice versa*.[27] This concept of the water-energy nexus has drawn great attention as both water and energy scarcity is becoming increasingly severe.[6,28–30] Thus, in this review, water and energy generation advances will be discussed in the same context with a focus on materials and structural innovation in developing sorbents and devices for moisture-enabled water and energy generation. By having alongside discussion on moisture-enabled water and energy generation technologies, the correlation between these two technologies from the perspective of materials design and engineering can be grasped. As summarised in Fig. 1, the technologies of harvesting water and energy from moisture are found to be rooted in the interactions between moisture and materials. These moisture/materials interactions are essentially determined by materials' water affinity, porosity, specific surface area, and thermal/electrical conductivity. Some of the emerging materials such as hydrogels and composites are well-suited for these two technologies. Such a correlation will enable good headway in these technologies as achievement in one technology will promote the progress of the other, considering the interdependency of energy and water commodities.

The structure of this review is organized as follows. First, the development of AWH technologies, especially sorbent-assisted AWH is discussed, including mechanisms behind the moisture/sorbent interaction, advanced sorbents emerging in recent years, strategies of engineering materials to boost the water generation performance and energy efficiency, and also recent water generation systems. Next, the technologies developed to harvest moisture-enabled energies, such as heat batteries, actuators, and electricity generators, are introduced, delving into the mechanisms and materials' engineering behind these technologies. Thereafter, the intrinsic connection and key principles in material design for water and energy generation from moisture are summarized. Finally, the future challenges and direction for wide and large-scale applications of these moisture-enabled water and energy generations are presented.

2. Water harvesting from moisture

Atmospheric water harvesting (AWH), as one of the decentralized strategies for freshwater generation, has the potential to provide flexible, distributed, community-managed, off-grid access to safe potable water, especially in areas where water scarcity is geographically or economically presented.[12] There are three common ways for AWH, including (1) fog collection by using large nets to capture water droplets suspended in air, (2) cooling air below its dew point to condense and collect water, and (3) sorbent-assisted harvesting where a sorbent or desiccant is employed for AWH. Compared with fog collection and air cooling, sorbent-assisted harvesting demonstrates superiority in terms of applicability to a wide variety of climates and geographies, water production, and energy efficiency.[15,19]

2.1 Overview of sorbent-assisted atmospheric water harvesting

Sorbent-assisted AWH primarily includes two stages: sorption and desorption. At the sorption stage, the sorbent captures moisture or water vapor and separates it from air. During the

Ghim Wei Ho received her PhD in semiconductor nanostructures at the Nanoscience Centre, University of Cambridge in 2006. She is a professor at the Department of Electrical and Computer Engineering at the National University of Singapore (NUS). She leads the sustainable smart solar system research group working on fundamental and applied research on nano-systems with emerging low dimensional nanomaterials, interfacial interactions, and hybridized functionalities for energy, environment, electronics, and healthcare.

This journal is © The Royal Society of Chemistry 2023

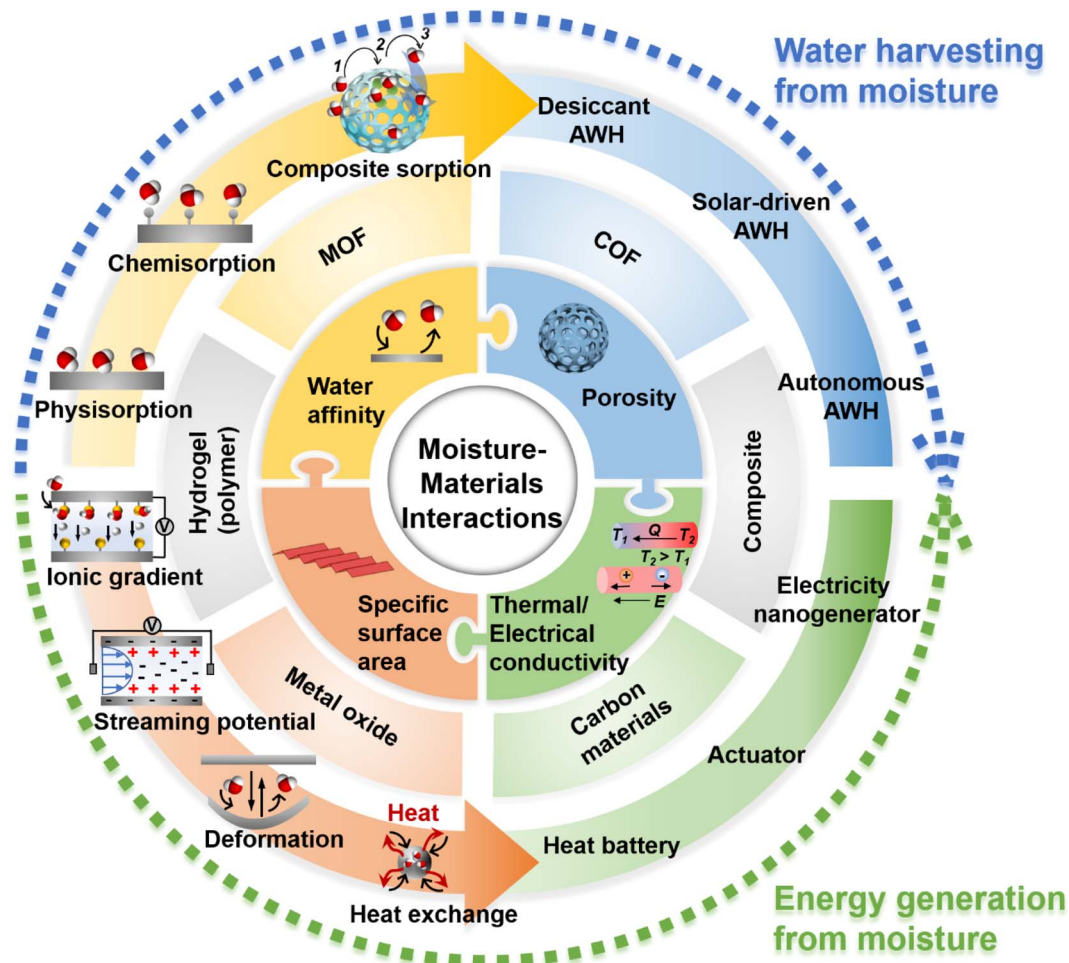*J. Mater. Chem. A*, 2023, **11**, 12456–12481 | **12457**

Fig. 1 Overview of moisture–enabled water and energy generation technologies that are reviewed in this article.

desorption stage, the sorbent is heated to release the vapor into an enclosed area to create local conditions with high humidity levels. This in turn reduces the sensible cooling requirement and the corresponding specific energy consumption for vapor condensation, especially under arid conditions.[31] The theoretical water production of the sorbent-assisted AWH is the difference between the sorption capacity under the sorption condition and the remaining water in the sorbents under the desorption condition. The energy requirement for sorbents to release water and to be regenerated during the desorption process determines the energy efficiency of the devices, and also defines the possibility to utilize renewable energy, such as solar light for AWH. Choosing a suitable sorbent is crucial to improve the AWH performance in terms of *e.g.*, sorption capacity, regeneration temperature, as well as the adsorption/desorption rate. The primary merits expected of a model sorbent include (1) large water sorption capability at a defined temperature and relative humidity (RH), (2) low regeneration temperature, ideally less than 100 °C to utilize solar energy or low-grade waste heat, and (3) a rapid sorption/desorption rate.[32] Other characteristics such as thermal and mechanical stability, non-toxicity, accessibility, and cost, should also be considered when

choosing AWH sorbents. Together with the appropriate choice of sorbents, structural design innovation at a device level would enhance the utilization of renewable energy, synergistically bolstering water production and energy efficiency.

This section will focus on strategies of material and structural design for improving sorbents toward water-productive and energy-saving AWH. First, mechanisms underlying the interaction between moisture and the sorbents are examined, followed by the discussion of materials' properties desirable for AWH, aiming to provide a fundamental understanding of AWH sorbents. Then, advances in developing AWH are elaborated with focus on emerging sorbents that have effectively addressed long-standing challenges faced by traditional sorbents (*e.g.*, limited sorption capacity, applicable humidity range, and high energy consumption). Also, innovations to boost the efficiencies of water production and energy consumption, including the integration of photothermal materials and structures as well as stimuli-responsiveness into AWH are summarised. Finally, various sorbent-assisted AWH systems spurred by these material and structural innovations are reviewed, such as desiccant-AWH, solar-driven AWH, and autonomous AWH.

12458 | *J. Mater. Chem. A*, 2023, **11**, 12456–12481

This journal is © The Royal Society of Chemistry 2023

2.2 Mechanisms underlying moisture/sorbent interactions

Sorbents, discussed in this paper, can be broadly categorized into two groups, namely adsorbents and absorbents. Adsorbents do not change chemically or physically in the presence of water vapor, whereas absorbents undergo chemical or physical change when they absorb water.[12] Correspondingly, the process of capturing moisture by the sorbents can be classified into adsorption and absorption. Generally, solid sorbents are adsorbents and adsorption tends to be a surface phenomenon, while liquid sorbents are absorbents and absorption is a bulk phenomenon. The moisture capture by the liquid sorbents such as high-concentration solutions of inorganic salts (e.g., $CaCl_2$,[33,34] $LiCl$,[35,36] and $LiBr$[37,38]) and ionic liquids,[39-41] is an absorption process where the water vapor diffuses into the liquid sorbents driven by the difference in the vapor partial pressure between the air and the surface of liquid sorbents. Solid sorbents such as silica gels, zeolites, activated alumina, and conventional composites capture moisture molecules in the air through physical adsorption (or physisorption), chemical adsorption (or chemisorption), or composite sorption (Fig. 2).[42]

2.2.1 Physisorption.

Physisorption occurs when moisture is bonded to the sorbent surface by weak van der Waals forces, and is an exothermic and reversible process (Fig. 2a). Thus, physical sorbents commonly feature low adsorption enthalpy, low activation energy, high adsorption/desorption rate, excellent reversibility, and stable cycle performance. The sorption capacity of the physical sorbents largely depends on the surface area, and commonly used physical sorbents include conventional porous sorbents with high specific surface areas, such as silica gels, activated carbon, zeolites, and aluminophosphates.

The sorption/desorption capacity of the porous sorbents can be evaluated from their sorption isotherms which present the equilibrium moisture uptake or loss at different water vapor pressures (or RH) and temperatures.[43] Fig. 2b shows six types of isotherms according to the classification of the International Union of Pure and Applied Chemistry (IUPAC). Type I isotherms are normally observed in hydrophilic microporous structures, like activated carbons, and zeolites. In a Type I isotherm, steep water uptake is presented at very low p/p_0 (or RH) as a result of monolayer sorption or micropore (<2 nm) filling induced by the strong gas–solid interaction between water vapor molecules and the porous materials. The water uptake approaches a limiting value as RH increases because it is determined by the accessible micropore volume rather than the surface area. Type II and III isotherms are depicted by the physisorption of most gases on nonporous or microporous (50–100 nm) sorbents. For Type II, the strong gas–solid interaction allows monolayer adsorption at low RH, and unrestricted monolayer–multilayer adsorption occurs as RH increases further. As for Type III, the water uptake is very low at low RH due to the weak gas–solid interaction or strong hydrophobicity. As RH increases the adsorbed molecules start to cluster around the most favorable sites on the porous structures, leading to an increase of water uptake at high RH. As the favorable sites are finite for Type III sorbents, the water
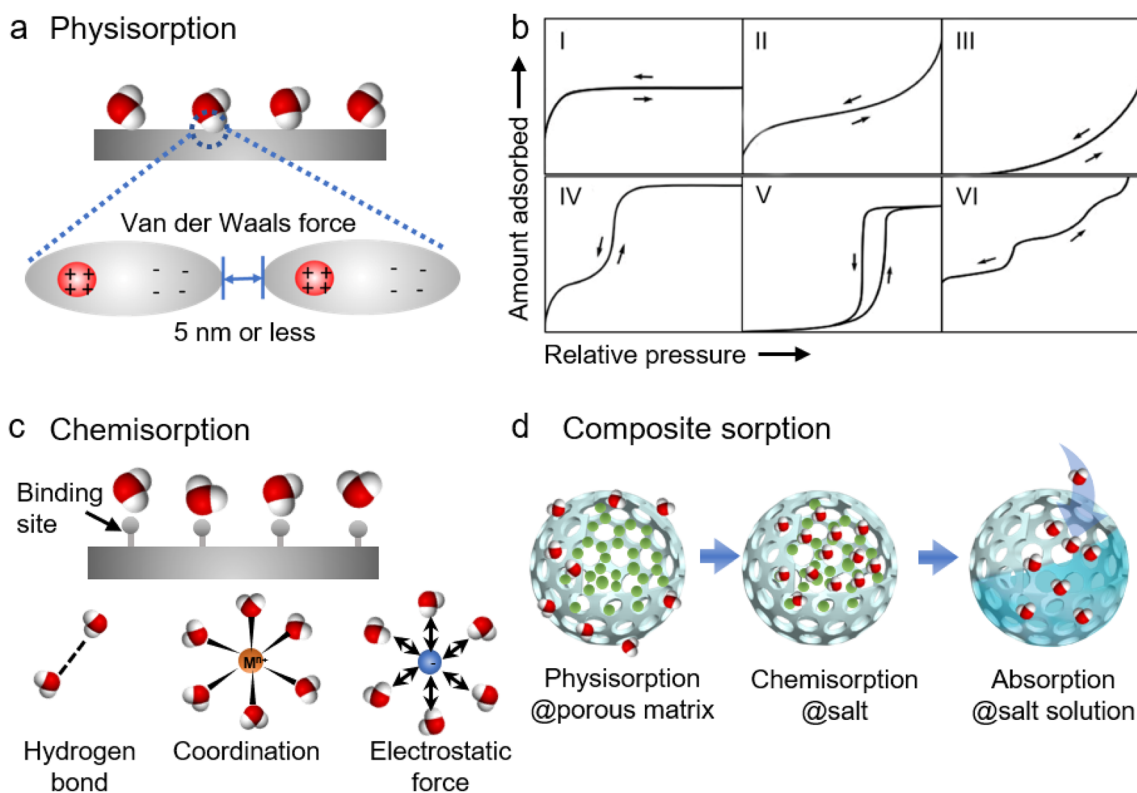

Fig. 2 Mechanisms behind interactions between moisture and sorbents: (a) physisorption; (c) chemisorption; and (d) composite sorption. (b) Six types of isotherms describing the physisorption of porous sorbents.

This journal is © The Royal Society of Chemistry 2023

J. Mater. Chem. A, 2023, **11**, 12456–12481 | **12459**

uptake remains finite even at the saturation pressure (*e.g.*, $p/p_0 = 1$), and they differ from Type II sorbents where the water uptake seems to increase without limit. Type IV isotherms are observed in hydrophilic mesoporous (2–50 nm) sorbents in which the sorption processes involve monolayer coverage induced by the strong gas–solid interaction, multilayer adsorption, and mesopore filling due to capillary condensation that occurs when the pore size is above a critical diameter, D_c. Capillary condensation refers to the phenomenon where vapor condensation occurs in a pore at a pressure less than the saturation pressure of the bulk liquid. The pore's critical diameter D_c can be estimated by using[44]

$$D_c = 4\sigma T_c / (T_c - T)$$

where $\sigma = 0.28$ nm is roughly the size of the water molecule, T is the temperature, and $T_c = 674$ K is the bulk critical temperature for water. At room temperature ($T = 298$ K), the D_c is estimated to be 2 nm. This indicates that when the pore size is below 2 nm, a reversible and continuous pore filling due to monolayer or cluster adsorption will occur. However, when the pore size is above 2 nm, the pore filling occurs due to capillary condensation. As this pore filling is irreversible, a hysteresis loop will appear on the isotherm curve.[45,46] Type V isotherms are seen for hydrophobic microporous and mesoporous sorbents. Type VI isotherms are representative of layer-by-layer adsorption on highly uniform nonporous surfaces.

According to the sorption isotherms, Type III sorbents are not good candidates for AWH sorbents because their water uptake starts at high RH and the sorption capacity is quite limited even at saturated vapor pressure. Though sorbents showing isotherms with Type I, II, and IV characteristics can work for moisture adsorption at low RH, they require lots of energy or high temperature to release the captured moisture. Type V sorbents, on the other hand, are regarded as ideal sorbents for AWH because of their S-shaped or step-shaped isotherms that allude to large water uptake and release through relatively small temperature or pressure gradients and warrant large sorption capacity with low energy consumption.[15,31,32]

2.2.2 Chemisorption. Chemisorption is caused by the formation of strong chemical bonding (*e.g.*, hydrogen bonding,[47,48] coordination effect,[49,50] and electrostatic interaction[51]) between moisture and the sorbent surface (Fig. 2c), and is slow, irreversible, and often requires high activation energy. But compared to physical sorbents, chemical sorbents are superior in their sorption capacity, for example, the water uptake of typical chemical sorbents such as hygroscopic salts (*e.g.*, LiCl, LiBr, CaCl$_2$, Ca(NO$_3$)$_2$, and MgSO$_4$), can be more than 1 g g^{-1}.[52,53] The moisture capture process of most hygroscopic salts is essentially a hydration reaction between the salt ions and water vapor. At the molecular level, both water and salts are polar, and when moisture interacts with salts, cations will be attracted to the negatively charged end (oxygen atom side) of water molecules, while anions will be pulled to the positively charged end (hydrogen atom side). As a result, chemical bonding, specifically the electrostatic interaction is established,

which then seizes the water molecules. Polymers, such as poly(acrylic acid) sodium salt (PAAS),[54,55] poly(diallyl dimethylammonium chloride) (PDDA),[56,57] and chloride-doped polypyrrole (PPy-Cl)[58] also have high sorption capacity because these polymers usually have many hydrophilic functional groups like –OH, –COOH, and –NH$_2$ that would form hydrogen bonding with water molecules. The coordination effect is often observed in the interaction between water molecules and many transition metal-containing coordination complexes.[59,60]

Similar to physical sorbents, the sorption capacity of chemical sorbents strongly depends on the surface area, where a larger surface area means more active sites to take up moisture. As the water molecules diffuse into the chemical sorbents, some sorbents may undergo significant volume expansion and agglomeration, which would impede mass/heat transfer and degrade sorption/desorption. Another major concern about the use of hygroscopic salts for AWH is deliquescence. Most hygroscopic salts have a low deliquescence relative humidity (DRH), for example, LiCl and CaCl$_2$ have a DRH of 11% and 29% at 30 °C, respectively.[32] Above DRH, deliquescence will occur which suggests the potential risks of liquid leakage and reactor corrosion when using hygroscopic salts for AWH.

2.2.3 Composite sorption. Composite sorption applies to the sorbents that are formulated with chemical sorbents dispersed within a porous matrix. The incorporation of chemical sorbents significantly enhances the sorption capacity, while the physical porous sorbents boost the sorption rate and effectively prevent the volume expansion, agglomeration, and even liquid leakage of the chemical sorbents.[61] The moisture sorption process of composites can be broken down into a series of processes: first, moisture is captured by the porous matrix due to the hydrophilic pore surface or pore structure; second, the hydration reaction occurs due to the interaction between chemical sorbents and the water molecule; third, with the increase in time or RH, deliquescence of some chemical sorbents like hygroscopic salts occurs to form a liquid sorbent that continues moisture adsorption until an equilibrium of water vapor pressure is reached in a diluted salt solution (Fig. 2d). Desorption is a reverse process involving solution evaporation, salt crystallization, salt dehydration, and vapor escape. This composite sorption process may concurrently or sequentially involve physisorption, chemisorption, and bulk absorption, which reveals the way how most sorbents work for AWH *i.e.*, sorption mechanisms can evolve or transform[62] and couple. This is also disclosed in the recent AWH sorbent innovations (more details will be discussed later). Classic composite sorbents include diverse combinations of porous sorbents and hygroscopic salts, such as LiBr@silica gel,[63] LiCl@silica gel,[64] LiBr/LiCl@silica gel,[65] CaCl$_2$@silica gels,[66] MgCl$_2$@activated carbon,[67] and CaCl$_2$@activated carbon.[68] The sorption capacity and sorption rate have been found to depend on the type and amount of the loaded hygroscopic salts, the water affinity, size, distribution, and the volume of the pores within the porous sorbents, as well as the manufacturing methods.[69–72]

2.2.4 Materials' properties for sorption. Based on the moisture/sorbent interaction mechanisms discussed above, the material properties to be considered when selecting or

12460 | *J. Mater. Chem. A*, 2023, **11**, 12456–12481

This journal is © The Royal Society of Chemistry 2023

designing sorbents for AWH can be summarised as follows: (1) material affinity towards water vapor, which affects the sorption capacity and is also strongly related to the lowest relative humidity where sorbents can work; (2) specific surface area, which signifies the number of sorption sites available on sorbents; (3) pore features including pore size, distribution, and volume, which dictate the types of sorption/desorption isotherms, speed of mass exchange, and also the sorption capacity; and (4) thermal conductivity which facilitates heat exchange and the corresponding sorption/desorption. Thus, at the materials' level, approaches that could adjust these properties would be effective strategies to endow sorbents with desirable features for AWH applications.

Surface functionalization is one of the effective methods to enhance the materials' affinity towards water vapor, where materials' surfaces can be modified to possess favourable functional groups to adsorb moisture. For example, functionalizing inorganic mesoporous carbon with amino-containing molecules such as poly(N-izopropylacryl amide) has resulted in a moisture adsorption capacity that is 7.2 times greater than that of the commercial silica gels.[73] The presence of oxygen-containing functional groups such as –COOH contributes to the water affinity of many carbon materials, which can be increased by oxidation treatment. Aside, an enhanced oxidation process has been shown to increase the O/C ratio of graphene oxide by 33%, which has led to a sorption capacity increase from $0.51\ \mathrm{g\ g^{-1}}$ to $0.61\ \mathrm{g\ g^{-1}}$.[74] Similarly, the oxidation of activated carbon has been found to create copious functional groups on its surface, hence resulting in a moisture sorption capacity larger than that of commercial silica gel. Besides the creation of functional groups, the enhancement of the moisture uptake has also been attributed to specific surface area and pore volume augmentation.[75] By optimizing the preparation conditions such as the activation temperature and time, and $ZnCl_2$ impregnation ratio, the specific surface area of activated carbons can reach $1893.6\ \mathrm{m^2\ g^{-1}}$, which, together with the microporous structures created, has resulted in a Type V isotherm and moisture sorption of $0.56\ \mathrm{g\ g^{-1}}$. Designing the pore structure of sorbents is another effective strategy to control the sorption/desorption behavior. A hierarchical porous aluminosilicate has been found to outperform commercial zeolite 3A and silica gel at both low and high RHs. This has been attributed to the chemically modified sorption sites, and also the hierarchical porous structures where both mesopores and micropores exist in a highly ordered hexagonal structure. This ordered structure endows the aluminosilicate with good stability, while the hierarchical meso- and micro-pores afford abundant sorption sites, and more importantly, they facilitate water vapor diffusion in the sorbents.[76] Furthermore, metal or activated carbon with high thermal conductivities has been mixed into the sorbents to improve the heat transfer properties of sorbents. For example, by employing activated carbon as the porous matrix to host silica gel and LiCl, the thermal conductivity of the composite can reach $0.253\ \mathrm{W\ m^{-1}\ K^{-1}}$, almost 1.6 times that of silica gel.[77] Besides that, increasing the packing density, for example, by compressing loose particle sorbents can enhance the thermal conductivity by 3 times.[78]

In addition to consideration of materials' properties, it is also beneficial to instil innovations that could help lower energy consumption or engage renewable energy both at the materials and device levels. In the next section, recent advances in sorbent-assisted AWH will be introduced, where strategies adopted to improve the performance of the sorbents and energy efficiency will be discussed.

2.3 Advances in sorbent-assisted AWH

2.3.1 Emerging sorbents for AWH. Fig. 3 summarises the emerging sorbents used for AWH in recent years, which include metal–organic frameworks (MOFs), covalent organic frameworks (COFs), hydrogels, and advanced composites. These advanced sorbents possess numerous attributes such as large surface areas, structural and compositional tunability, accessible pores, physicochemical stability, etc.

2.3.1.1 MOFs. Metal–organic frameworks (MOFs) are porous coordination networks constructed by linking inorganic clusters with organic linkers.[79,80] The wide variety of inorganic clusters, organic linkers, and network topologies used in constructing MOFs, confers MOFs with a high degree of chemical and structural tunability for diverse applications, such as gas storage and separation, catalysis, biomedical applications, electronic and ionic conduction, and sensors.[81–83] Together with other remarkable features such as high specific surface areas and high pore volumes, MOFs have been widely accepted as promising AWH sorbents.[31,44,84–86] As mentioned, evolving and coupling sorption/desorption mechanisms govern the recent developments of AWH sorbents. MOFs capture water molecules through multiple mechanisms including (1) chemisorption, whereby water molecules are adsorbed on the metallic clusters, (2) monolayer-multilayer or cluster adsorption, and (3) irreversible pore filling due to capillary condensation.[44] MOF-74 has a Type I isotherm with a preferred moisture uptake at a low relative pressure (e.g., 10% RH), and its moisture adsorption stems from the strong water interaction with open metal ions, e.g. Ni^{2+}, Mg^{2+}, Co^{2+}, and Zn^{2+}.[87] Similar phenomena are also observed in HKUST-1 where the high water affinity of the open metal sites, Cu^{2+}, contributes to its moisture uptake at around 25% RH.[88] The chemisorption and cluster adsorption function together for the moisture adsorption of UiO-66.[89] The pore size of MIL-101(Cr), ranging from 2.9 to 3.4 nm, is larger than that of MOF-74 and UiO-66 ($\sim$1 nm) and greater than the critical pore diameter ($D_C = 2$ nm) for capillary condensation, or irreversible pore filling. The pore size of MIL-101(Cr), in addition to the chemisorption related to open metal sites, contributes to the S-shaped (or step-shaped, Type V) isotherm and sorption capacity up to $1.4\ \mathrm{g\ g^{-1}}$.[90]

It is crucial to develop sorbents that can facilitate atmospheric water harvesting in arid and desert climates since other freshwater generation techniques (e.g., fog capture and dewing) and conventional sorbents such as silica gels, zeolites, and hygroscopic salts tend to be energy intensive and impractical. In recent years, Yaghi and colleagues have devoted to creating efficacious devices that can capture moisture in extremely dry air and simultaneously exploit the abundant solar energy in arid
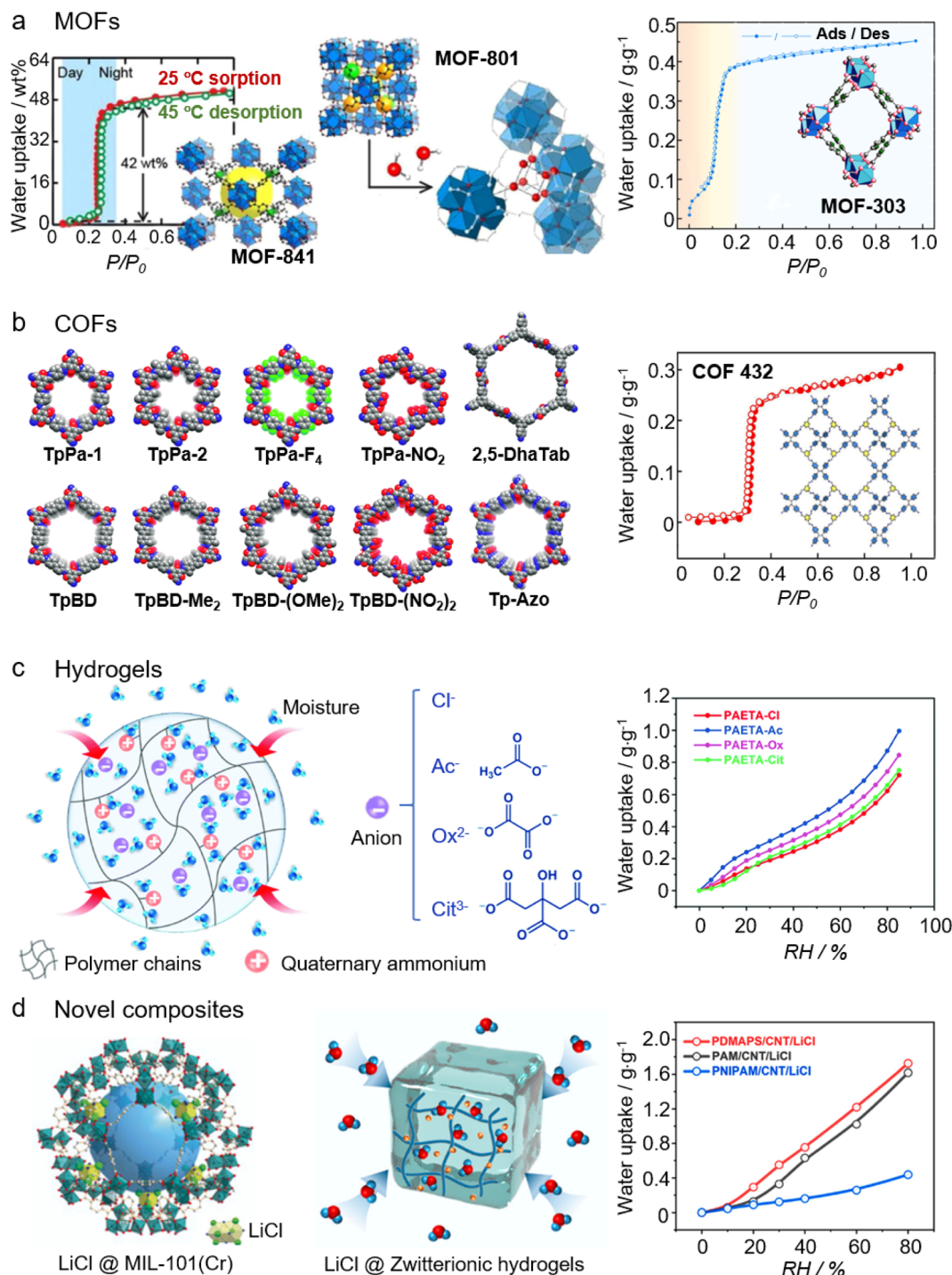
This journal is © The Royal Society of Chemistry 2023

J. Mater. Chem. A, 2023, **11**, 12456–12481 | **12461**

Fig. 3 Four types of emerging sorbents used for AWH: (a) structure and water isotherm of MOF-841 (left) and MOF-801 (middle). Printed with permission.[91] Copyright 2014, American Chemical Society. Structure and water isotherm of MOF-303 (right). Printed with permission.[96] Copyright 2021, the American Association for the Advancement of Science. (b) A library of Schiff-base COFs (left). Reproduced from ref. 114 with permission from the Royal Society of Chemistry. Structure and water isotherm of COF-432 (right). Printed with permission.[115] Copyright 2020, American Chemical Society. (c) Structure (left) and water isotherms (right) of PAETA-X hydrogels, where X is an anion and can be varied as Cl$^-$, Ac$^-$, Ox^{2-}, and Cit^{3-}. From, ref. 118 used under the Creative Commons CC-BY license. (d) Structure of the LiCl@MIL-101L(Cr) composite sorbent (left). Printed with permission.[121] Copyright 2020, Wiley. Structure of LiCl@Zwitterionic hydrogels (middle) and water isotherms (right) of LiCl@Zwitterionic hydrogels (PDMAPS), LiCl@PAM, and LiCl@PNIPAM. From, ref. 122 used under the Creative Commons CC-BY license.

areas to minimize the energy cost for freshwater generation. The key component of these devices are MOF-based sorbents (Fig. 3a), *e.g.* MOF-841 [Zr$_6$O$_4$(OH)$_4$(MTB)$_2$(HCOO)$_6$],[91] MOF-801 [Zr$_6$O$_4$(OH)$_4$(fumarate)$_6$],[92,93] Co$_2$Cl$_2$BTDD[94] and MOF-303 [Al(OH)(PZDC), PZDC = 1*H*-pyrazole-3,5-dicarboxylate].[95,96] All these MOFs have S-shaped isotherms and exhibit capabilities to

12462 | *J. Mater. Chem. A*, 2023, **11**, 12456–12481

This journal is © The Royal Society of Chemistry 2023

harvest water up to 0.25–0.84 g g^{-1} at relatively low RH ($0.1 < p/p_0 < 0.4$). Moreover, these MOF-based sorbents can be dehydrated and regenerated at a low temperature (∼65 °C) that can be attained by solar irradiation. The thermal insulating nature of MOFs limits the sorption/desorption kinetics, which consequently restricts the sorption/desorption cycling number and hence, the water productivity. In 2022, Zhu's group reported a MOF-derived nanoporous carbon with a density of binding sites up to 40% and a pore size of ∼1 nm. By virtue of the minimized diffusion resistance, efficient solar-thermal heating, and high thermal conductivity, the sorption/desorption kinetics are accelerated. As such, the water productivity of the MOF-derived nanoporous carbon can reach 0.18 L kg^{-1} h^{-1} at 30% RH under one-sun illumination.[97]

When it comes to the practical application of MOFs for AWH, hydrolytic stability is the first consideration. Some MOFs may undergo hydrolysis or linker displacement which can weaken or even break the metal–ligand bond,[98] losing their hydrolytic stability for AWH. To enhance water stability, selecting appropriate linkers and metal ions is an effective strategy.[99] Linkers such as pyrazolate and imidazolate are favorable in forming water-stable MOFs.[100,101] Modifying the linker with different functional groups is also helpful in improving water stability. For example, non-polar functional groups could provide the steric shielding effect to effectively limit water diffusion to the metal nodes and thus improve stability.[102] Polar functional groups could also work as they are capable of drawing water away from the metal nodes.[103] Highly charged metal ions such as Zr^{4+}, Ti^{4+}, and U^{6+} tend to enhance hydrolytic stability as they are often highly coordinated to exert a steric shielding effect to protect MOFs from water attack. Also, the kinetic inertness of the metal ions plays a critical role in improving MOFs' water stability. For example, the water stability of the isostructural MIL-53 is found to be consistent with the inertness of the central metals.[104]

In addition to improving MOFs' water stability, selecting appropriate linkers and metals is widely sought to enhance their water harvesting performances. As mentioned, the uncoordinated or open metal sites are favourable for water binding, underpinning the sorption capacity of MOFs like HKUST-1 and MOF-74 (ref. 87 and 88) at a low relative humidity. Functionalizing metal clusters or the organic ligands of MOFs with various functional groups also helps to tune MOFs' moisture sorption behaviours. For example, decorating the Zr cluster in Zr(IV)-MOFs with functional groups having high water affinity can lead to a lower operating RH and higher water uptake.[105] The water uptake of CAU-10-X is found to be proportional to the size of the functional group, X, attached to the organic ligands.[106] Essentially, MOFs are porous solids, of which the moisture sorption behaviour can be determined by the porous structures. The pore size is found to play a more important role than the hydrophilicity in determining the sorption behaviour of MOFs. Owing to its ideal micropore size, the water uptake of MOF-801, despite not having any hydroxyl group, is much higher than that of its counterparts having hydroxyl groups (MOF-804 and MOF-805).[91] Modifying MOFs with hydrophilic functional groups can bring about an improvement in water uptake, but in some cases, the modification may also cause an increase in the pore size and the occurrence of capillary condensation. Capillary condensation will lead to a hysteresis sorption/desorption loop, which means that lower RHs or more energies are required for complete moisture desorption.

2.3.1.2 COFs. Covalent organic frameworks (COFs) are porous and crystalline polymers produced by covalently linked organic molecular building units with pre-designed geometry. Owing to their unique features such as low densities, high crystallinity, highly porous structures, large internal surface areas, regular pore structures, and flexibly tailored functionalities, COFs have been recognized for wide applications in the fields of adsorption, gas storage, and separation, catalysis, and optoelectronics.[107–111] Similar to MOFs, the water uptake behavior of COFs can be tuned by systematically adjusting chemical functionality and pore size.[112,113] A thorough study details the water uptake behavior of a series of chemically stable Schiff-based COFs (the left panel of Fig. 3b), which reveals the effect of functionality, surface area, and hydrophilicity-hydrophobicity on their moisture harvesting performance. Among these Schiff-based COFs, TpPa-1 without any functional groups decorating each COF pore shows excellent performance for water adsorption. It possesses an S-shaped sorption isotherm with a sorption capacity of 0.3 g g^{-1} and 0.45 g g^{-1} at 30% RH and 90% RH, respectively.[114] In 2020, Yaghi reported a new, 2D-linked framework, termed COF-432 [(ETTA)$_3$(TFB)$_4$] imine. This COF-432 exhibits attractive water sorption properties, including long-term stability upon water uptake/release cycling, a hysteresis-free S-shaped water sorption isotherm, and low heat of adsorption that allows for regeneration at low temperature or by using low-grade energy sources (Fig. 3b).[115] Distinct from MOFs where metal ions, especially heavy metal ions such as Ni^{2+}, Co^{2+}, and Cr^{3+}, are resting in the center of MOFs, COFs are composed of light elements (*e.g.*, B, C, N, O, and Si) linked together by strong covalent bonds. This metal-free nature of COFs can eliminate the concerns of the potential contamination of metal ion seepage into the freshwater collected. COFs are essentially porous solids formed by covalently linked organic clusters. Thus, functionalizing the organic units with various functional groups to control their hydrophilicity or pore structures is effective to improve the water harvesting performance of COFs.

2.3.1.3 Hydrogels. Hydrogels are networks of hydrophilic polymer chains that are physically or chemically crosslinked, characterized by numerous sites that interact with water molecules, *e.g.*, the hydrophilic/hydrophobic functional groups, the spaces between the network chains, micro- or macro-pores, and voids.[116] This allows for high hygroscopicity and hydration of the hydrogels. Together with their solid states, scalability, and compatibility with practical sorbent-assisted AWH device features, hydrogels, or hygroscopic porous polymers have recently become the focus of next-generation sorbents for AWH.[117] Fig. 3c shows one such hydrogel network with high hygroscopicity and hydration, which is formed by crosslinking quaternary ammonium monomers. Followed by an ion-exchange process, the anions in the hydrogel network can be varied to exhibit different moisture sorption behaviors.[118]

This journal is © The Royal Society of Chemistry 2023

J. Mater. Chem. A, 2023, **11**, 12456–12481 | **12463**

Similar to MOFs, water sorption of hydrogels supports multiple mechanisms, including chemisorption owing to the hydrogen bonding between hydrophilic functional groups and water molecules, physisorption by mono-/multi-layer adsorption, and capillary condensation due to the presence of nanopores. First principle density functional theory (DFT) calculations have been performed to estimate the energy required to bond water molecules to a hydrogel made from non-stoichiometric zinc oxide. The bonding energy is initially 1.04 eV when a few water molecules are introduced into the hydrogel structures, and then it decreases to 0.7 eV as the number of water molecules increases. The initial high and the decreased bonding energies correspond to hydroxylation (one form of chemisorption) at the early phase of sorption, and the water cluster or layer formation due to physisorption.[119,120]

It is noted that the kinetics of hydrogel sorption is distinct from that of other solid sorbents like silica gels and MOFs because vapor transport and liquid transport are coupled with the sorption of hydrogel-based sorbents. When exposed to a humid environment, water vapor first enters the hydrogel through the interconnected gaseous micropores. Next, due to the presence of a vapor pressure difference, the vapor will diffuse from the center to the walls of micropores, leading to sorption on the liquid–gas interface of the micropores. At the same time, the liquid diffuses through the nanopores of the hydrogel network as a result of the water chemical potential difference between the wet and dry regions of the hydrogel network, which will result in the expansion of the hydrogel network and the shrinkage of the micropores. Through model calculation and experimental verification, the vapor transport is found to be significant at the initial state when the water content is low and the gaseous micropores occupy a large volume ratio of the hydrogel, while the sorption kinetics tends to be dominated by the liquid transport as the sorption and the liquid transport proceed. This study also demonstrates that for faster kinetics, a thinner hydrogel with a higher shear modulus (to enhance the liquid transport) and appropriate porosity (to balance the vapor and liquid transport) are preferred.[123]

For hydrogels in their pure form without any added hygroscopic additives (*e.g.*, inorganic salt or organic additives), the sorption capacity mainly relies on surficial hydrophilic functional groups and porous structure, and is often less than 1 g g^{-1} even at high RH.[118] However, the hydrogel network is an exceptional platform for diverse material modification and functionalization,[124,125] which allows for the addition of various hygroscopic salts and photothermal materials to the hydrogel, imparting high sorption capacity and energy efficiency to the composites. Details about the functionalization of hydrogels and the development of composite sorbents will be discussed in the next section on advanced composites.

2.3.1.4 Advanced composites. Conventional composite sorbents are typically prepared by distributing hygroscopic salts (*e.g.*, CaCl$_2$ and LiCl) in porous matrices like silica gels and activated carbon, with aims to increase the water sorption capacity, sorption/desorption kinetics, and meanwhile, avoid salt leakage.[61] As many innovative sorbents like MOFs and hydrogels have emerged in recent years, the development of composite sorbents also gives rise to new combinations of sorbents, striving to boost AWH performance.

Owing to their large pore volume, huge specific surface area, robust pore structures, and tunable chemical features, MOFs are new and promising porous matrix materials to load large amounts of salt to achieve high sorption capacity. Hygroscopic salts such as CaCl$_2$ and LiCl have been confined in various MOF matrices and without exception, the sorption capacities of these salt@MOF composites have improved.[121,126–128] For example, the sorption capacity of LiCl@UiO-66 with a salt loading of 35 wt% is six times that of UiO-66 at 60% RH at 25 °C.[126] Likewise, confining LiCl in MIL-101(Cr) (left panel of Fig. 3d) changes the sorption isotherm and increases the sorption at 30% RH to 0.3 g g^{-1}. In contrast, a pure MIL-101(Cr) has a sorption isotherm where the inflection of water uptake appears at 40 to 50% RH, which indicates its negligible water uptake at low RH (*e.g.*, ≤30% RH).[121]

The amount of salts loaded in the rigid porous matrices is mainly determined by the total pore volume, and noting that excessive salt loading will lead to the overflow of salt solutions, also known as salt leakage. This means that even for MOF materials with huge pore volumes, the salt loading amount and hence the improvement in the sorption capacity is limited, especially when working at high RH. Different from the rigid porous matrices, hydrogels possess crosslinked and flexible networks of polymer chains that can host a large amount of water and salt solution, suggesting the feasibility of holding a significant salt content within hydrogels. The CaCl$_2$ mass loading has been reported to be as high as 4.0 g per gram of the polyacrylamide (PAM) matrix, exhibiting a sorption capacity of 1.2 g g^{-1} at 60% RH.[129] CaCl$_2$ and binary salts (LiCl and CaCl$_2$) have been incorporated inside the biopolymeric alginate network with a loading percentage of 78 wt% and 86 wt%, respectively. These salts@alginate composites exhibit excellent sorption performance over a wide range of humidities: the sorption capacity can be 1.0 g g^{-1} and 5.6 g g^{-1} at 26% RH and 90% RH, respectively.[130,131] Zwitterionic polymers possess oppositely charged cationic and anionic functional groups alongside their polymer chains. This characteristic endows a unique salt-responsive anti-polyelectrolyte effect, more specifically, the introduction of salt species into the polymer network screens the self-association effect between oppositely charged functional groups and allows the polymer chains to stay stretched even in a high concentrated salt solution (middle and right panels of Fig. 3d). This distinctive anti-polyelectrolyte effect not only helps to coordinate more salt species, but by creating stretched conformations of polymer chains, it also improves the liquid transport (*e.g.*, water solubility and swelling) in hydrogels. The liquid transport is the key to boosting the sorption/desorption kinetics in hydrogel-based materials. Such composite sorbents of a salt@zwitterionic hydrogel exhibit a water sorption capacity of up to 0.62 g g^{-1} at 30% RH within 2 hours and 1.3 g g^{-1} at 60% RH.[122,132] Besides the commonly used inorganic salts, organic hygroscopic salts are also incorporated into the hydrogel network to enhance their sorption capacity. For example, introducing polypyrrole chloride (PPy-Cl) into the hydrogel network of poly(*N*-isopropyl

12464 | *J. Mater. Chem. A*, 2023, **11**, 12456–12481

This journal is © The Royal Society of Chemistry 2023

acrylamide) (PNIPAAM) has boosted the sorption capacity from 0.2 (ref. 133) to 6.7 g g^{-1}.[58]

In addition to MOFs and hydrogels, other nanosized porous materials such as activated carbon fibers,[134–136] and nanosized carbon hollow spheres,[137] are also employed as the matrix for hygroscopic salts. The water sorption capacities of these salt@nanosized porous structures are higher by virtue of nanosized porous structures with large surface areas to host copious well-distributed salts and reduced barriers for mass/heat exchange during the sorption and desorption process. Moreover, many of these nanosized porous materials such as carbon-based materials have high thermal conductivity, which will benefit the sorption/desorption kinetics.[19,77]

2.3.2 Engineered sorbents for energy efficient AWH. The materials-by-design paradigm highlights the rational material design strategies to develop materials with desirable properties and functions. Specifically, for the development of AWH sorbents, engineering sorbents with photothermal and responsive materials can endow sorbents with explicit features such as light–heat conversion and responsivity to external stimuli. These features will effectively boost AWH's energy efficiency.

2.3.2.1 Nanostructured photothermal materials. Incorporating nanostructured photothermal materials into the sorbents is an effective strategy to improve the energy efficiency of AWH, not only because of the engagement of renewable solar
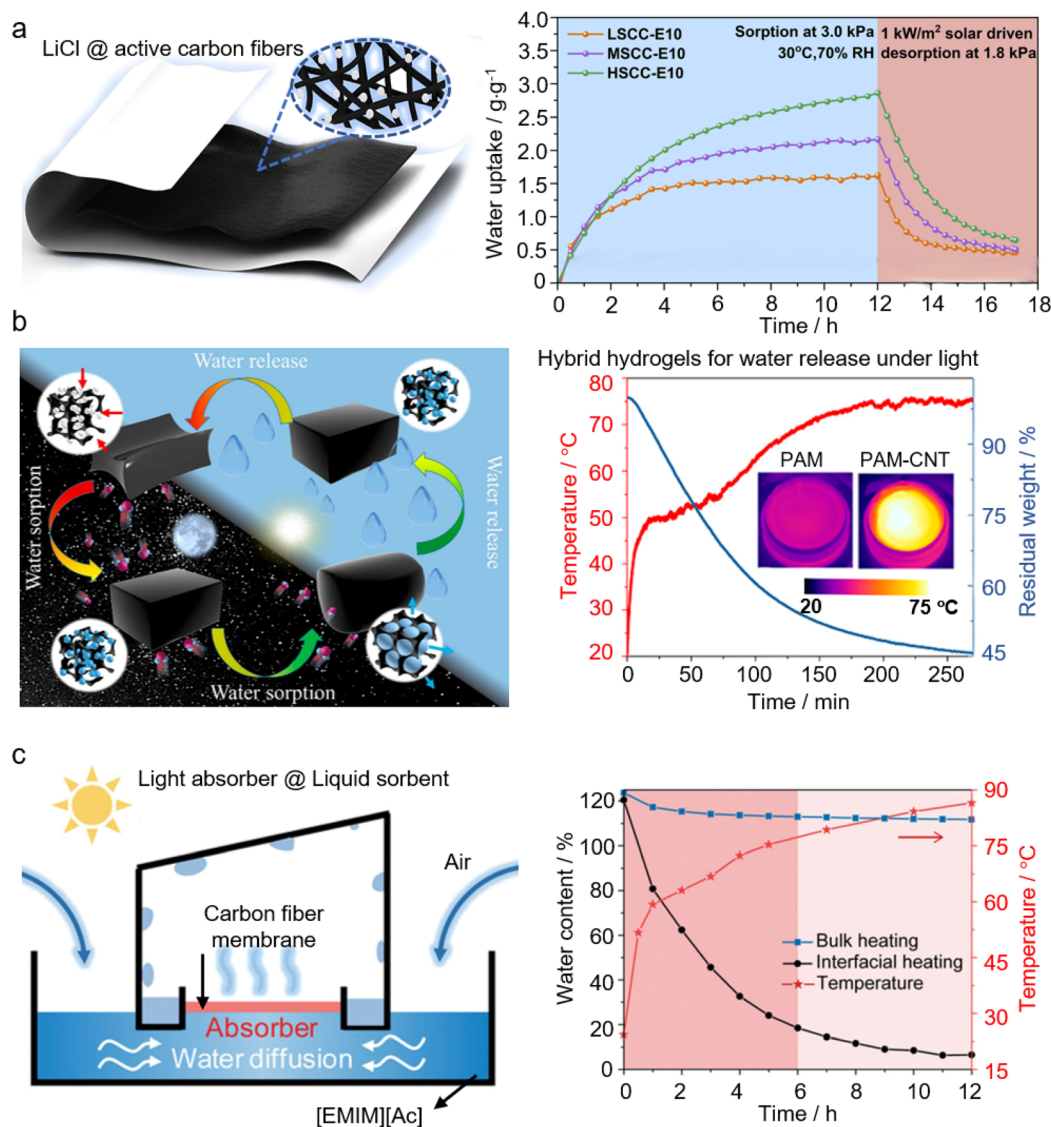

Fig. 4 Application of photothermal materials in sorbent-assisted AWH: (a) structure of HSCC-Ex, where LiCl is distributed on the active carbon fiber felts (left). Dynamic sorption and solar-driven desorption performances of composites with different salt loadings. From, ref. 134 used under the Creative Commons license. (b) A CNT-hybrid hydrogel that adsorbs moisture at night and releases water during the day (left). Changes in the surface temperature and the water loss with light illumination (right); the insets are the IR images of the CNT-free and CNT-hybridized hydrogels under one sun irradiation. From, ref. 129 used with permission of ACS publication. (c) Schematic illustration of a continuously working interfacial solar-driven atmospheric water generator (left).The temperature of the absorber surface and water content change between interfacial solar heating and conventional solar bulk heating over time (right). Printed with permission.[40] Copyright 2020, Wiley.

This journal is © The Royal Society of Chemistry 2023

J. Mater. Chem. A, 2023, **11**, 12456–12481 | **12465**

energy for sorbent regeneration (and water release) but also the utilization of solar energy with high energy conversion efficiency.[8,138] By doing so, the localization of thermal energy conversion at the air/liquid interface is ensured to reduce thermal losses and improve the energy conversion efficiency of sorbent regeneration. In 2018, Wang's group reported a bilayered AWH device, where the bottom layer is a salt-loaded fibrous membrane to capture moisture from air while the top layer is a photothermal layer of CNTs to convert solar energy to heat and release the captured moisture upon sunlight illumination. This bilayered device can work in an arid climate with the humidity down to 15% RH and release water under regular or even weakened sunlight (*e.g.*, 0.7 kW m^{-2}).[139] Fig. 4a shows a composite sorbent consisting of active carbon fiber felts as a photothermal matrix to host LiCl. This composite sorbent has achieved an ultra-high sorption capacity of 2.83 g g^{-1} at 70% RH, and the absorbed moisture can be released under one sun illumination. Nanostructured photothermal materials like CNTs are also infused into the hydrogel network to form a hybrid hydrogel network to exploit solar energy for AWH.[129,131,140] Fig. 4b shows one of the typical examples to illustrate the release of the collected water under solar irradiation from a CNT-infused hybrid hydrogel. It is worth noting that in such a hybrid hydrogel functionalized by photothermal materials, the energy efficiency improvement would be more significant because of the presence of a large proportion of intermediate water within the hydrogel network that effectively reduces the overall energy demand of vapor generation during the desorption process.[9,141] In addition to CNTs, many other nanostructured photothermal materials are found to play a role in solar-driven AWH, including novel nanoparticles,[142,143] graphene,[144] graphene oxide (GO),[145] carbon fibers,[134–136,146] nano-sized carbon hollow spheres,[137] carbon black or ink,[147–149] polypyrrole,[58,150] poly-pyrrole-dopamine (PPy-DA),[56,57,151] and others.

Nanostructured interfacial photothermal materials have also found innovative use in liquid sorbent-based AWH. Vast energy consumption is a well-known issue of AWH based on liquid sorbents, and pertinently, the progress in interfacial solar evaporation is promising to overcome this bottleneck. In 2019, Zhu's group demonstrated an AWH based on a high-concentrated liquid sorbent, of which the desorption process is expected to be energy-consuming. However, by placing a salt-resistant GO-based aerogel at the liquid–gas interface as a solar interfacial heater, desorption of the high-concentrated liquid sorbent can be achieved with a solar energy efficiency as high as 66.9%, and the device can produce freshwater of 2.89 kg m^{-2}·per day at about 70% RH.[34] In this device, the surface of the liquid sorbent is fully covered by photothermal materials, and freshwater is generated based on sequential absorption–desorption processes. By simply changing the photothermal materials (*e.g.*, the carbon fiber membrane) from full coverage to partial coverage over the liquid sorbent surface, as schematically shown in Fig. 4c, this AWH can change the working mode from sequential to simultaneous adsorption–desorption to continuously harvest water from atmospheric air.[40]

2.3.2.2 Stimuli-responsive polymers. The terms, stimuli-responsive, smart, or intelligent materials refer to materials that undergo a reversible phase transition accompanied by notable changes in shapes, volumes, transport of ions and molecules, wettability, and adhesion of different species in response to external physical, chemical, and/or biological stimuli.[152–154] Owing to their adaptivity and sensitivity to changes in the environment, smart polymers are playing an increasingly important role in manifold fields such as drug delivery, biology, medicine, biosensors, oil-gas industries, coatings, and textiles.[152–159] One of the most widely employed smart polymers is thermal responsive polymers which, in response to temperature, will swiftly change their physical and/or chemical properties. There are two types of thermal responsive polymers as shown by the phase diagram in Fig. 5a. If a homogeneous polymer solution starts to separate into heterogeneous phases above a critical temperature (defined as the lower critical solution temperature, LCST), this polymer is an LCST-type polymer. In contrast, if the phase separation happens below a critical temperature (referred to as the upper critical solution temperature, UCST), it is a UCST-type polymer.[153]

The most well-known and extensively investigated thermal responsive polymer is poly(*N*-isopropyl acrylamide), abbreviated as PNIPAAM. PNIPAAM is an LCST-type polymer, which undergoes a reversible phase transition from a hydrophilic coil state to a hydrophobic globule state when the temperature is elevated above its LCST at around 30–35 °C.[160] This means that when the temperature is lower than the LCST, PNIPAM is hydrophilic and it can adsorb and store water. Conversely, when the temperature is higher than the LCST, it becomes hydrophobic and starts to repel water out of its polymer network. This unique feature of PNIPAAM is reminiscent of ideal sorbents for atmospheric water harvesting. As reported, an ideal sorbent should preferably be temperature-sensitive; specifically, at a designated temperature, the water sorption capacity increases linearly with relative humidity (RH) in the sorption process, and drops steeply with increased temperature in the desorption process.[15] Fig. 5b shows the moisture sorption isotherms of a PNIPAAM interpenetrating polymer network (IPN) gel (the inset of Fig. 5b) at various temperatures.[133] It can be found that the moisture adsorption capacity grows rapidly with RH at low temperatures (<30 °C), and it drops significantly at temperatures above 35 °C. This remarkable change in the moisture adsorption capacity with temperature is attributed to the change of the PNIPAAM chains from hydrophilic to hydrophobic, which perfectly illustrates that it has great potential to function as a temperature-sensitive sorbent for atmospheric water harvesting.

Besides conferring temperature sensitivity, the innovative application of PNIPAAM in moisture sorbents can also revolutionize the freshwater collection method in AWH. Gaseous water is adsorbed by freeze-dried PNIPAAM gels and retained as liquid water in the water-swollen PNIPAAM hydrogels. The stored liquid water is oozed out of the hydrogels due to a temperature-triggered (>32 °C) change in the hydrophilicity/
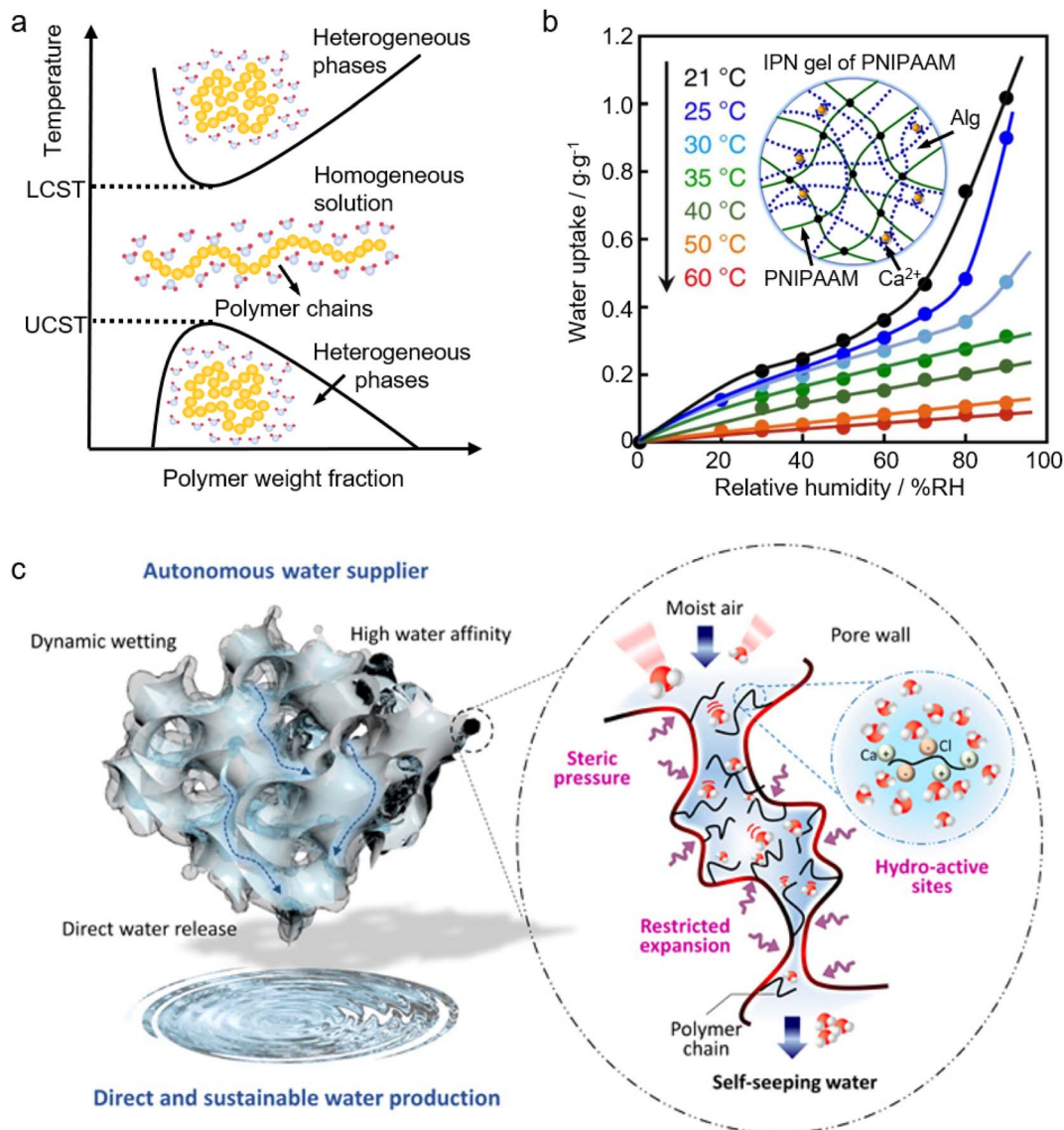
12466 | *J. Mater. Chem. A*, 2023, **11**, 12456–12481

This journal is © The Royal Society of Chemistry 2023

Fig. 5 Application of smart materials in sorbent-assisted AWH: (a) the phase diagram of a thermal responsive polymer. (b) Moisture-absorption isotherms of the IPN gels at various temperatures. The inset is the schematic structure illustration of the IPN gels. From, ref. 133 used under the Creative Commons CC-BY license. (c) The schematic illustration shows the structure of a PNIPAAM-MOF-hybridized matrix, where the hydro-active sites on polymer chains enable atmospheric moisture capture, and under steric pressure and restricted expansion, the polymer-MOF hybrid pore enables self-seepage for direct water harvesting from ambient moisture. From, ref. 142 used under the Creative Commons CC-BY-NC license.

hydrophobicity of the PNIPAM chains. This direct water oozing has successfully avoided the cumbersome water collection method used by a conventional sorbent-assisted AWH where the freshwater is collected by a multi-step process involving water vaporization (by heating the saturated sorbent) and the ensuing moisture condensation.[133] By incorporating hygroscopic materials such as MOFs and salts into PNIPAAM, the water sorption capacity can be significantly increased without an adverse influence on its water oozing behavior at its LCST.[58,133,142,145,161] In a PNIPAAM-MOF-hybridized matrix (Fig. 5c), the sorption capacity can hit 6 g g^{-1} at 90% RH, and strikingly, freshwater generation in this hybrid is autonomous and continuous. The captured moisture will spontaneously seep from the hybrid matrix to offer a freshwater supply.

Importantly, it can sustain its sorption performance, without having to halt the sorption to proceed with desorption to collect water and regenerate the sorbents.[142] Apart from the gel form, PNIPAAM also paves a way for AWH through diverse forms such as polymer brushes,[162,163] fibers,[164,165] and thin films or membranes.[166–168]

Many polymers have an LCST close to that of PNIPAAM, around the human physiological temperature, such as poly(N,N-dimethyl acrylamide) (PDEAAM),[169] poly(N-vinyl caprolactam) (PVCL),[170–172] poly(methyl vinyl ether) (PMVE),[173] and poly(2-isopropyl-2-oxazoline) (PIZO).[174] Other polymers having different ranges of LCST include PEG (polyethylene glycol-based) copolymers (20–85 °C), derivatives of 2-oxazoline (PO$_X$) (23–75 °C), and some natural polymers such as methyl cellulose

This journal is © The Royal Society of Chemistry 2023

J. Mater. Chem. A, 2023, **11**, 12456–12481 | **12467**

(MC, 40 °C), hydroxypropyl cellulose (HPC, 45 °C), and hydroxypropylmethyl cellulose (HPMC, 69 °C).[160] It should be noted that the LCST can be further tuned by varying the length of the polymer chain,[175,176] the tacticity of polymers,[177] the end group,[178,179] and the type and ratio of the incorporated co-polymer,[180,181] or by adjusting a synthesis condition like pressure.[182] This LCST tunability as well as the discovery of natural LCST-type polymers offers the feasibility of AWH devices working at different temperatures and eliminates toxicity concerns. Some smart polymers not only respond to one specific external stimulus but can respond to dual-/multi-stimuli. The stimuli-responsive behavior of smart polymers stems from different functional groups within the polymer chain that respond to different stimuli. Combining several functional moieties within one polymer has been proven effective to create dual-/multi-stimuli-responsive smart polymers.[183–185] Currently, although few investigations have conducted on employing dual-/multi-stimuli-responsive smart polymers in AWH, we can anticipate their promising applications. For example, incorporating light-sensitive functional moieties into a PNIPAAM gel will mobilize a light switch in addition to the temperature switch for this smart sorbent, which would boost its AWH performance, especially in cold seasons or regions.

2.4 Sorbent-assisted AWH systems

Benefiting from advances in sorbent engineering and development, many sorbent-assisted AWH systems have recently been developed. In accordance with the energy required for the desorption process, these systems can be classified into three modes, that is, desiccant AWH, solar-driven AWH, and autonomous AWH. Among them, desiccant AWH and solar-driven AWH conform to a similar moisture sorption and desorption cycle to extract atmospheric water. The major difference between them lies in the energy input to release the moisture and regenerate sorbents whereby external heaters are required for desiccant AWH, while solar energy is exploited *via* photo-thermal materials for solar-driven AWH. Distinct from desiccant and solar-driven AWH, autonomous AWH does not necessarily follow the water sorption/desorption cycle. Instead,
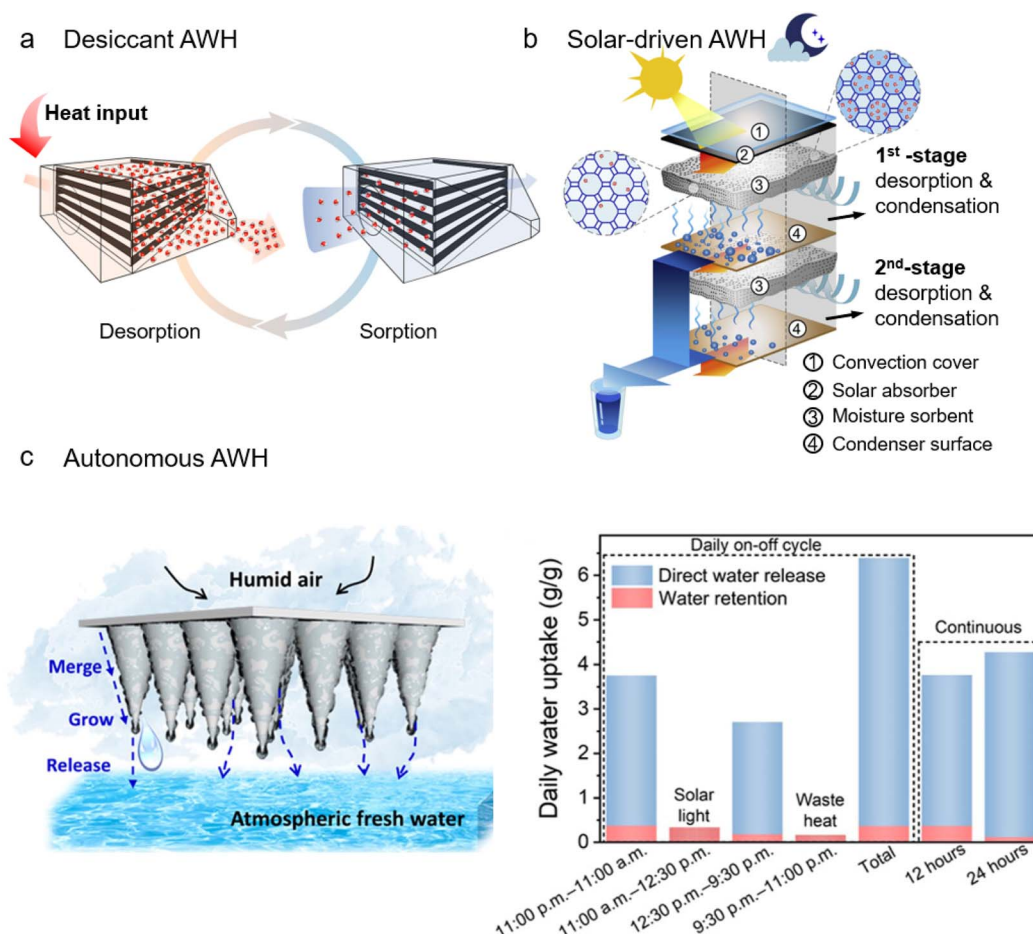

Fig. 6 Sorbent-assisted AWH systems developed due to innovations in material and structural designs: (a) desiccant WHC, where the water captured is released by heating the sorbent bed. From, ref. 95 used with permission of ACS publication. (b) Solar-driven AWH with a dual-stage design, where desorption in the top stage is driven by the heat generated from a solar absorber under sunlight, while in the bottom stage, besides solar light, desorption is also driven by the latent heat released from the condensation in the top stage. Printed with permission.[189] Copyright 2020, Elsevier Inc. (c) Autonomous AWH with a geometry of a cone array (left), and its water harvesting in a continuous daily on−off cycle. From, ref. 142 used under the Creative Commons CC-BY-NC license.

12468 | *J. Mater. Chem. A*, 2023, **11**, 12456–12481

This journal is © The Royal Society of Chemistry 2023

autonomous AWH exploits responsive and adaptable materials as sorbents to enable autonomous water release and achieve uninterrupted regeneration of hydro-active sites for continuous sorption.

A typical desiccant AWH is presented in Fig. 6a, in which a combination of heating strips and fans is implemented for forced convective heating during the desorption process.[95] During convective heating, the sorbent bed can be heated to 80–120 °C to trigger the release of water vapor and sorbent dehydration for use in the next sorption cycle. The sorption/desorption cycle can be programmed as desired. With the use of MOF-303, a sorption/desorption cycle can transpire within minutes, which effectively takes advantage of the initial fastest stage of the sorption process and maximizes the number of cycles within a day to boost water productivity. Consequently, the device can deliver water of 1.3 L kg^{-1} day^{-1} in an arid environment (32% RH), and at extremely low RH (10% RH), the produced water can be 0.7 L kg^{-1} day^{-1}. Besides the heating strips, other electrical heating materials can also be employed, for example, carbon scaffolds,[186] carbon fibers,[187] and metal foam.[188] Commonly, these electrical heating materials also work as a backbone to support sorbents, imparting an intimate contact and hence localized electrical heating at the heater/sorbent interface. Compared with traditional heating methods, the use of localized electrical heating can realize rapid and uniform heating, leading to complete and fast water desorption. At 28–32% RH, a water productivity of 1.95 L kg^{-1} day^{-1} can be reached.[186] At 60–88% RH, the water harvesting cycles can be performed eight times over 24 hours and generate water of 2.2 L kg^{-1} day^{-1}.[188]

Solar-driven AWH has been extensively developed because it can absorb light energy for the desorption process without requiring additional heat or electricity. Many solar-driven AWH systems with diverse structures have been developed, including the single basin,[190,191] the multi-shelves,[192] and the tubular solar still.[193,194] By virtue of its simple configuration, the single basin has been widely applied in solar-driven AWH.[85,92,93,134,195] In these solar-driven AWH systems, moisture sorption happens during nighttime to take advantage of natural cooling. During daytime, the basin is closed and the sun rays are allowed to pass through the basin cover to heat the sorbents, causing the adsorbed moisture to be released and then condensed on the basin walls that are attached to an active or passive cooler. Most solar-driven AWH works in one sorption/night-and-desorption/day cycle. Using only natural cooling and ambient sunlight as the energy source, 0.1–0.25 L kg^{-1} day^{-1} of water can be produced by these solar-driven AWH systems in an arid environment (10–40% RH).[85,92] If an active condenser is added, the water vapor condensation process can be greatly enhanced, leading to daily water productivity of 2.8 L kg^{-1} day^{-1}.[93] A recent innovative solar-driven AWH has demonstrated, without an active condenser, manifesting enhanced water productivity by a heat loss reduction tactic. Fig. 6b shows a dual-stage device with the capability to recycle the latent heat of condensation to improve water productivity. Specifically, during the solar-driven desorption process, the water vapor released from the first stage (close to the solar absorber) is condensed at the passive condenser surface, accompanying the condensation heat release. The released condensation heat is collected and exploited by the second stage for desorption. The daily water productivity reaches 0.77 L kg^{-1} day^{-1}, which is twice that of a single-stage device.[189]

Fig. 6c shows an autonomous AWH system comprising a responsive polymer-MOF-Au-mixed matrix with a cone array geometry, in which directional migration of water droplets can be realized by the gravitation effect to accelerate water removal and refresh the sorbent active sites.[142] An all-day water harvesting process can be realized in such an autonomous AWH system. As shown in the right panel of Fig. 6c, 3.74 g g^{-1} water has been extracted from the ambient air (90% RH) during the first 12 hours of moisture exposure, of which 90 wt% is directly released from AWH without activating any heat or solar-driven desorption. The remaining 10 wt% can be fully released *via* solar light. All in all, this autonomous AWH system can yield 6.39 g g^{-1} of water in a daily cycle. Note that in addition to solar light, waste heat in the environment can also be used to dehydrate the matrix, suggesting its independence from sunlight and its self-sufficiency in delivering freshwater.

3. Energy harvesting from moisture

More than 70% of the Earth's surface is covered by water. When the Sun's irradiation hits the Earth's surface, water becomes the largest carrier of energy on the Earth.[13] Atmospheric water or moisture is formed through water evaporation, which contains large-scale and inexhaustible energy because the liquid-to-gas phase transition has absorbed a large amount of heat from the sun and ground radiation. In light of the development of nanomaterials and nanotechnology, many technologies to harvest energy from water have materialized in recent years, with the emerging hydrovoltaic technology being one striking example.[26] Hydrovoltaic technology refers to electricity generation through the interaction between nanostructured materials with water in its diverse forms, including flowing liquids, moving droplets, fluctuating waves, as well as floating moisture. Moisture is abundant and ubiquitous in air and the interaction with materials (*e.g.*, moisture sorption) can be regulated and heightened, as illustrated in Section 2. This suggests that energy harvesting from moisture possesses the characteristics of AWH like flexible, distributed, and off-grid accessibility, and promises to supply decentralized, uninterruptable, clean, and green energy.[6,26,196,197] Here, technologies developed in recent years to harvest energy from moisture or gaseous water are reviewed, where moisture takes on multiple roles as an energy contributor or as a mediator in various energy conversions. Specifically, these technologies include moisture-enabled electricity generation (direct moisture-electricity generation and evaporation-driven electricity generation), moisture-responsive actuation, and moisture-mediated heat battery.

3.1 Moisture-enabled electricity generation

Nanomaterials usually have a high exposure of their atoms on the surfaces, allowing for substantial interactions with water

This journal is © The Royal Society of Chemistry 2023

J. Mater. Chem. A, 2023, **11**, 12456–12481 | **12469**

molecules. The generation of electricity through significant interactions with moisture has been observed in a variety of nanomaterials, which can be explained primarily by two suggested mechanisms, namely the ionic gradient and stream potential. According to the underlying mechanisms, moisture-enabled electricity generation can be categorized into direct moisture-electricity generation (MEG) and evaporation-driven electricity generation (EEG), respectively.

3.1.1 Ionic gradient. Fig. 7a schematically shows the mechanism of the ionic gradient to explain direct moisture-electricity generation. The ionic gradient mechanism often occurs in nanomaterials with a prebuilt gradient of functional groups, *e.g.*, the hydrophilic oxygen-containing groups of –COOH. These functional groups often have high water affinity to absorb moisture. The interactions with moisture will weaken or break the polar chemical bonds within functional groups,

dissociating the functional groups to release mobile ions, like the protons (H^+) released through the dissociation of –COOH. Thus, when nanomaterials with a prebuilt gradient of functional groups are exposed to moisture, a gradient of the ionic concentration will be established. Driven by this ionic gradient, the mobile ions released during the hydration process will move from the high-concentration region to the low-concentration region, resulting in electricity generation.

The mechanism of ionic gradient underlies many of the so-called direct moisture-electricity generation (MEG) systems where electricity is generated by the interactions of ubiquitous moisture and nanomaterials with ionized groups.[24] Qu's group has pioneered studies on MEG systems. The left panel of Fig. 7b shows a typical moisture-electricity generator consisting of a pair of electrodes and reduced graphene oxide (rGO) with a chemical-gradient structure, *e.g.*, the gradient of oxygen-
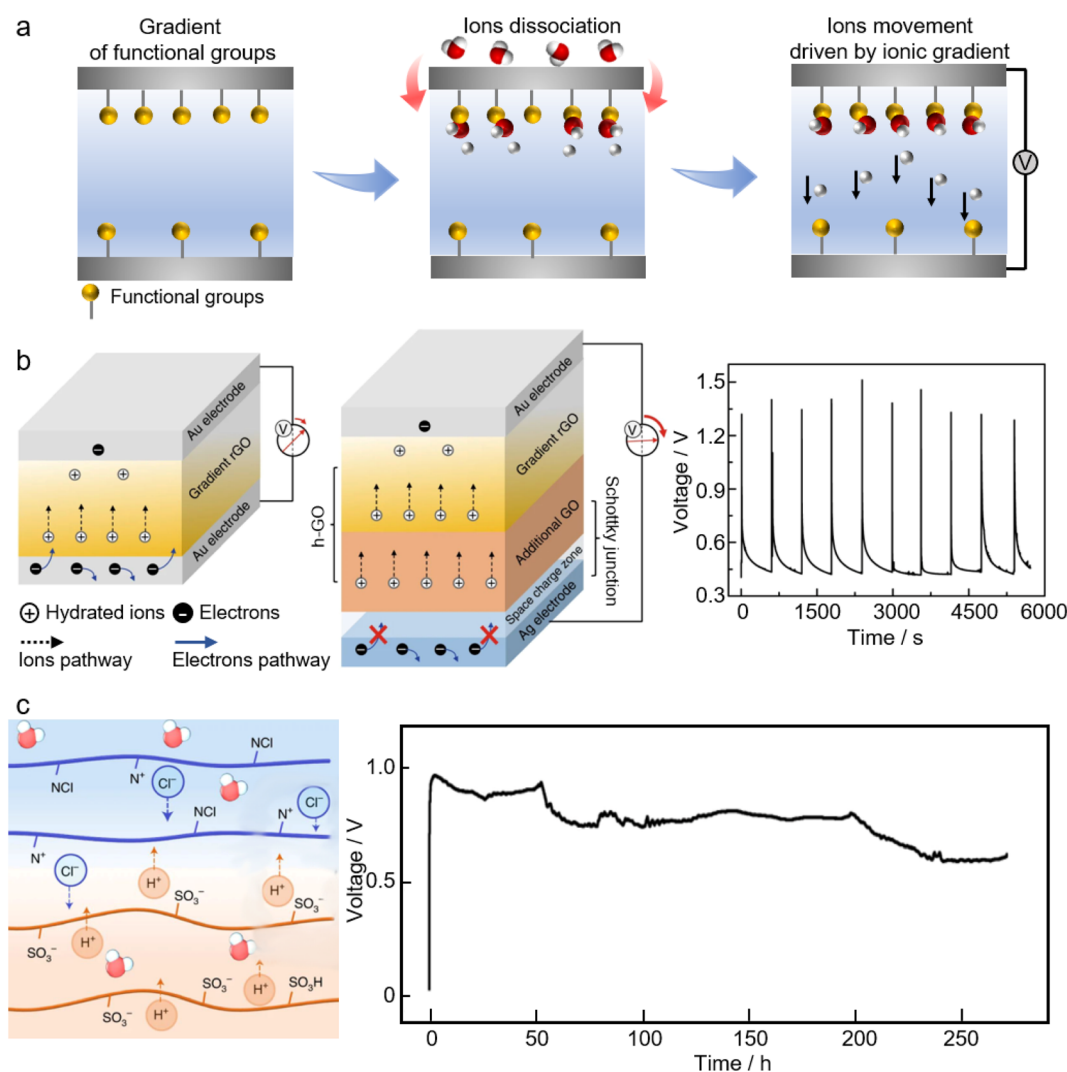

Fig. 7 (a) The ionic gradient mechanism of moisture–electricity generation. (b) Schematic of moisture–electricity generators composed of a single chemical gradient structure (left) and with an additional heterogeneous (GO) layer as well as asymmetrical electrodes (middle). The electrical pulse output in response to humidity variations (right). From, ref. 198 used the under Creative Commons CC license. (c) Schematic illustration of moisture-electricity generation in a bilayer of polyelectrolyte films (left) and the voltage output of this moisture-electricity generator (right) that is sustained for 258 h under atmospheric conditions of ∼15–30% RH and 25 ± 5 °C. Printed with permission.[199] Copyright 2021, Springer Nature Limited.

12470 | *J. Mater. Chem. A*, 2023, **11**, 12456–12481

This journal is © The Royal Society of Chemistry 2023

containing functional groups.[198] Once exposed to air, the functional groups of the MEG active materials start to release free H^+ due to the ionization of water molecules. Due to the prebuilt gradient of functional groups, the concentration of free H^+ will be higher at the bottom, driving H^+ to move towards the top, thus producing voltage and current. Furthermore, this chemical gradient-based MEG can be modified by adding an extra layer of graphene oxide (GO) to feed more mobile ions for electricity generation. Besides, employing asymmetrical electrodes with well-aligned work functions makes the electrons flow in the external circuit consistent with the proton migration within the MEG materials (the middle panel of Fig. 7b). Such a modification can result in a high-voltage MEG with the output approaching 1.5 V.[198]

The key to such a MEG system is to create an ionic gradient, *e.g.*, by prebuilding a gradient of functional groups. This chemical gradient can be prebuilt within materials by diverse methods, including electrochemical treatment,[200] air plasma treatment,[201] laser treatment,[198,202–205] and concentration-controlled electrodeposition.[206,207] Many materials are found to be MEG active, such as graphene quantum dots,[204] graphene oxides,[198,202–204,208–210] porous carbon films,[201] and polymers.[205–207,211,212] Besides, instituting a water gradient within materials is a simple but effective method to generate an ionic gradient for MEG. For example, sealing the bottom of the device from moisture and exposing the top to moisture will cause a water gradient and hence an ionic gradient increasing from the bottom to the top, consequently yielding an electrical output.[213] An asymmetrically moisturizing MEG system can be readily achieved by employing two electrodes with different air permeabilities.[214,215] Depending on the nature of the MEG active materials and the structural geometry, the electrical output of MEGs can be either instantaneous pulses in response to humidity variations, or a continuous sustained power output.[21] Restricted by the low concentration of free ions (due to the low coverage of ionized groups in thin-filmed MEG materials) and the fast charge transfer (prompted by the porous structures of MEG materials), the generated voltage or current of typical MEGs tends to occur as electrical pulses that would collapse within tens of seconds (the right panel of Fig. 7b). By increasing the film thickness of the graphene oxides to hundreds of micrometers, or adopting materials having a large volume of functional groups, the pulses can be changed into a continuous electrical output.[208,215–217] One example is a MEG device that is made from two asymmetrical electrodes and a porous thin film of protein nanowires. In humid air, a self-maintained water gradient is presented along the thickness of the protein nanowire network, which, combined with ample functional groups bonded to the protein nanowires and the electrode asymmetry, contributes a power supply that is continuous and can last for more than two months. In most cases, the ions responsible for MEG share the same polarity. Recently, inspired by the trans-membrane potential across the lipid bilayer of many cells, MEG devices featuring an oppositely charged heterojunction have emerged to deliver continuous power, where ions with opposite electrical polarities are engaged for moisture-induced electricity generation (Fig. 7c).[199,218–220]

3.1.2 Streaming potential.

When a liquid makes contact with a solid, an electric double layer (EDL) is formed at the liquid–solid interface.[221,222] This EDL, as shown in Fig. 8a (left panel), is composed of a surface layer firmly adsorbed on the solid (known as the Stern layer) and a diffusion layer that is rich in counter-ions. The boundary between the Stern layer and the diffusion layer is the shear plane, and the distance between the shear plane and the nearest bulk liquid region is the Debye length, in which the concentration of counter-ions is decreasing from the shear plane to the bulk liquid. The liquid flow in a solid channel will transport the counter-ions along with the liquid and form an electrical potential and current which is defined as stream potential or stream current (the right panel of Fig. 8a).[26] For channels with a nanoscale size close to the Debye length of the liquid (typically ranging from 1 to 100 nm (ref. 223)), the EDL will overlap and have more counter-ions in the narrow channel, resulting in a heightened stream potential or current. This phenomenon has been reported for porous materials like stacked carbon nanoparticles,[224–226] silicon nanowire arrays,[227] natural wood,[228] or transition metal oxide nanowires.[229,230] The electrical output of the moisture-enabled electricity generator based on the streaming potential depends on the hydrodynamics within the device. The voltage (or current) of such devices can be continuous without any interruption once the liquid flow in the nanochannels is sustained.

Inspired by the transpiration process of plants, evaporation-driven electricity generation is developed, where the water evaporation process is leveraged to offer uninterrupted liquid flow for streaming potential. Fig. 8b and c show the evaporation-driven electricity generator made from aluminium oxides and its electrical output.[231] A large volume of nanopores presented in these stacked aluminium oxide nanoparticles are ideal nanochannels for streaming potential and also help to drive water through the capillary pressure.[231,232] Similar evaporation-driven electricity generation has been observed on carbon nanoparticles,[224,225] biomaterials,[233] and zinc oxide films.[234] Besides water evaporation, engineering porous materials with heterogeneous hygroscopicity, for example, by depositing hygroscopic inorganic salts at one end of the device, has proven to be effective in facilitating the liquid flow from the salt-deposited end to the salt-free end, hence resulting in electricity generation.[149,235,236]

3.2 Other forms of moisture-enabled energy conversion

In addition to moisture-enabled electricity generation, immense efforts have been made to harness moisture in air to play a crucial role in a variety of energy conversions, harvesting mechanical and thermal energies.

3.2.1 Moisture-responsive actuation.

In nature, there are many examples illustrating shape deformation in response to humidity in the environment. For example, the opening/closing of pinecones, and the expansion/shrinking of spider silk,[237] bacillus spores,[238] wood,[239] and paper[240] take place as a result of humidity changes. With the wisdom borrowed from nature, many efforts have been devoted to developing water-responsive

This journal is © The Royal Society of Chemistry 2023

J. Mater. Chem. A, 2023, **11**, 12456–12481 | **12471**

materials that promise high energy actuation,[241–243] through the expansion/contraction of these water-responsive materials in response to changes in humidity or a water/humidity gradient. Fig. 9a shows a moisture-responsive actuator made from a PEE-PPy polymer composite. This polymer composite can exchange water molecules with the environment to induce film expansion and contraction, leading to rapid and continuous locomotion powered by the humidity gradient. Besides the moisture-responsive flips, this polymer composite enables the attached piezoelectric elements to convert the moisture-induced mechanical energy into electricity.[242,244] Moisture-induced mechanical energy generation (or moisture-responsive

actuation) has also been observed in the networks or fibers of polymers,[80,243,245–248] fibers of graphene oxide and carbon nanotubes,[249–252] membranes of graphene oxide,[253] and composites of graphene/polymer, bacterial spores/polymer,[254] and MXene/cellulose.[255,256]

3.2.2 Moisture-mediated heat battery. The moisture adsorption and desorption process essentially involves heat exchange between materials and environments. Thus, the interaction between moisture and sorbents is often used for thermal storage and heat management. As shown in Fig. 9b (left), when moisture is driven away from the sorbents, the sorbents can be charged with the thermal energy from the
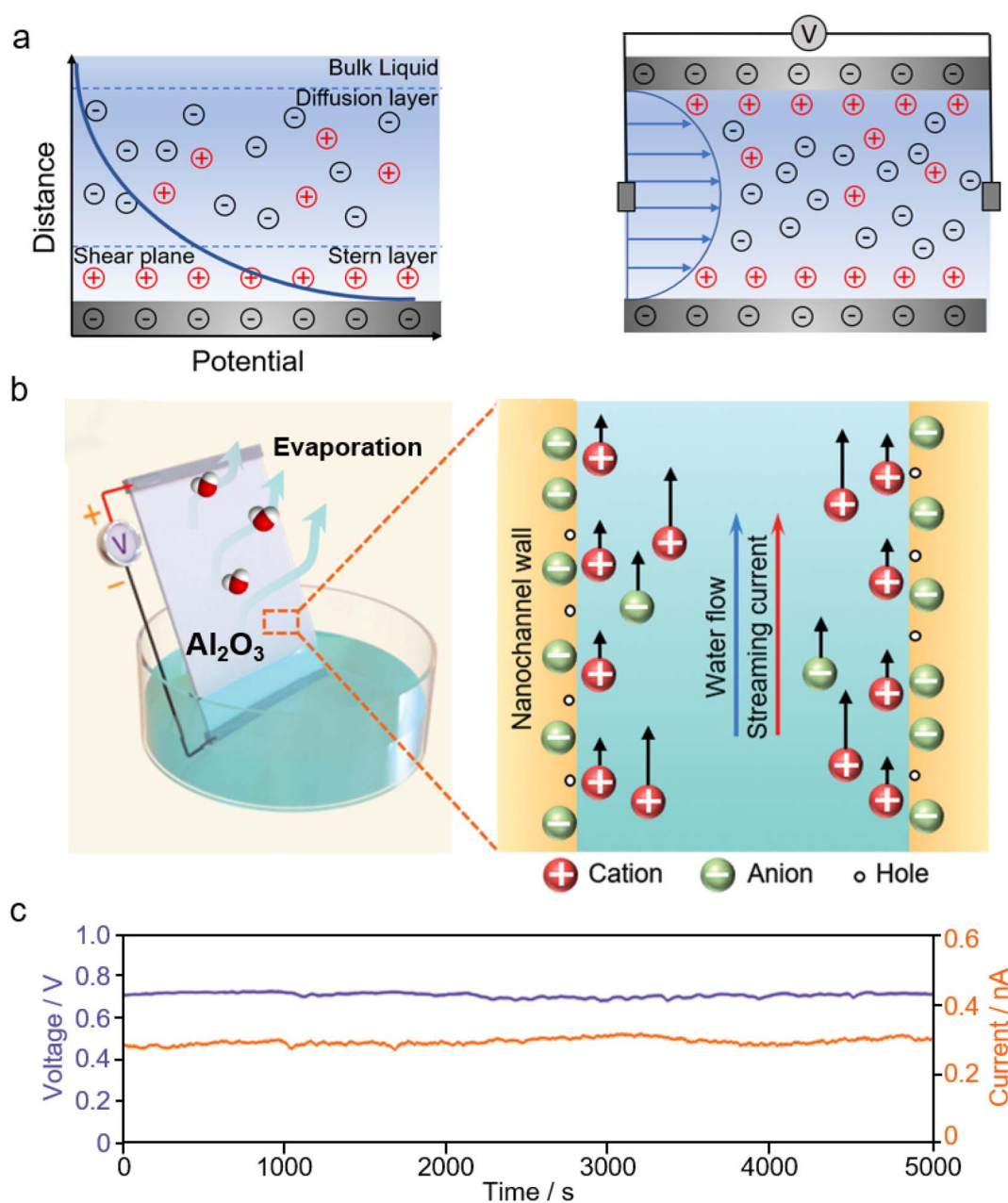

Fig. 8 (a) Schematic illustration of the electric double layer (EDL) formed at the liquid–solid interface (left), and streaming potential generation as a hydrodynamic flow within narrow channels. (b) Schematic illustration of the evaporation-driven electricity generator made from aluminium oxides and (c) its voltage and current output. From, ref. 231 used under the Creative Commons CC-BY license.
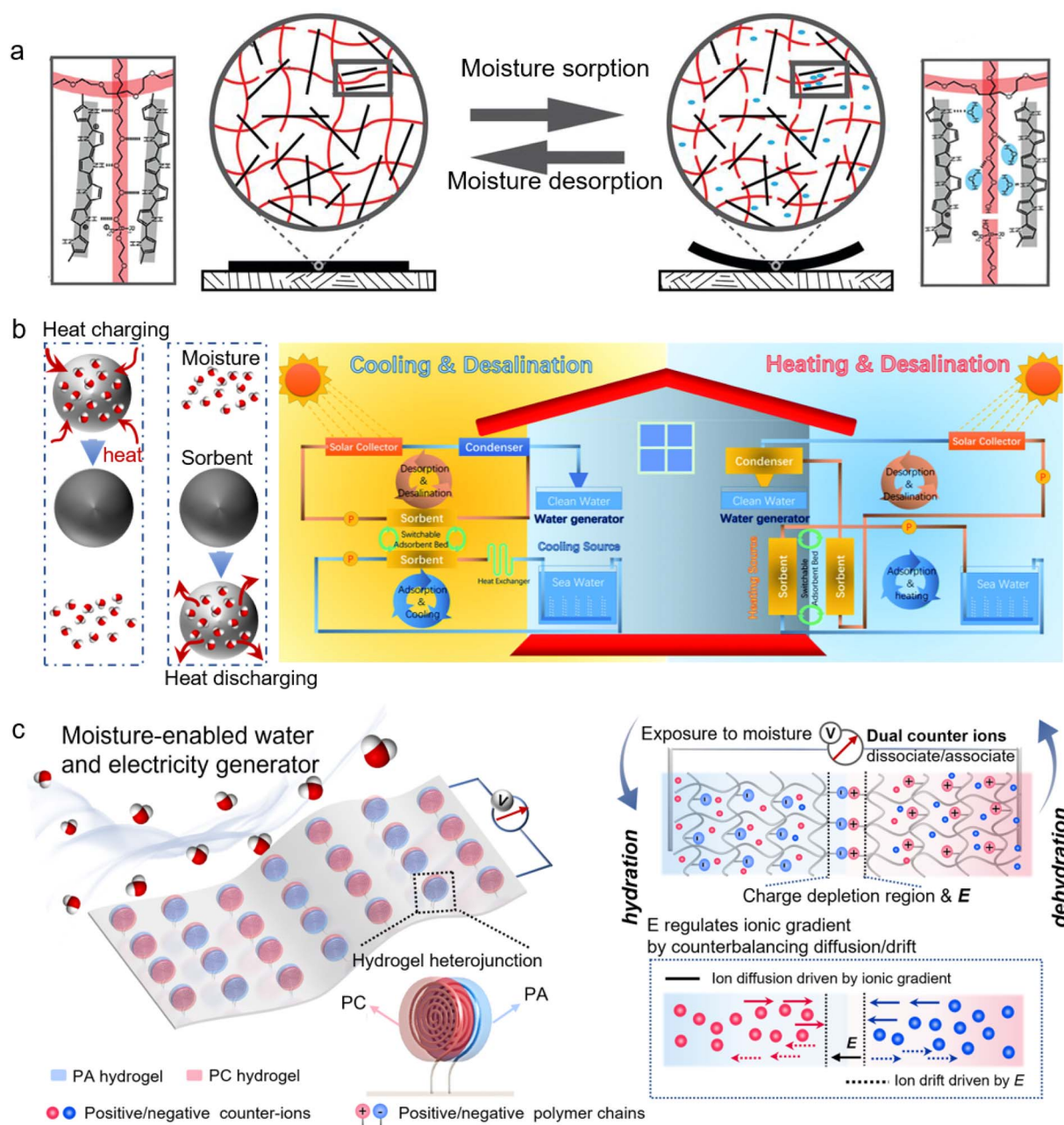
12472 | J. Mater. Chem. A, 2023, 11, 12456–12481

This journal is © The Royal Society of Chemistry 2023

Fig. 9 (a) A PEE-PPy composite film changes its structure in response to water sorption and desorption. Printed with permission.[242] Copyright 2013, the American Association for the Advancement of Science. (b) Heat charging and discharging as the moisture moves away from and into the sorbent (left). The conceptual design of combining a sorbent-based heat battery and desalination for switchable household heating and cooling (right). From, ref. 257 used under the Creative Commons CC-BY-NC license. (c) Schematic representation of a moisture-enabled electricity and water generator (MEWG) made from hydrogel heterojunctions consisting of two oppositely charged hydrogels: positively charged PC and negatively charged PA hydrogels. Printed with permission.[220] Copyright 2022, Elsevier Ltd.

environment. Conversely, when moisture is attracted to the sorbents, the charged thermal energy will be discharged back to the environment by a moisture sorption process.[258,259] This heat exchange can be performed in a controllable fashion and can be used for environmental heating and cooling. The moisture sorption of hollow SiO_2 spheres/LiCl composite sorbents can achieve a temperature lift of 20 °C. A heat battery system based on the SiO_2 spheres/LiCl composite sorbents, when combined

with seawater desalination, could be used for household thermal management, as shown in Fig. 9b.[257] In hot weather, the solar thermal energy is charged into the sorbent *via* a solar-driven desorption process, and in turn, during the moisture adsorption process, the energy is discharged to power seawater evaporation to cool the indoor environment. In cold weather, moisture adsorption is directly used for heating. Other means of tapping waste heat exchange include integrating

This journal is © The Royal Society of Chemistry 2023

J. Mater. Chem. A, 2023, 11, 12456–12481 | 12473

thermoelectric[260–262] or pyroelectric elements[6] into the moisture-mediated heat battery system to achieve electricity generation. Undeniably, these combinatory efforts of utilizing freely available moisture and waste heat to generate electricity can revolutionize the production of renewable energy.

3.3 Two-in-one water and energy harvesting from moisture

As discussed above, owing to the developments of new materials such as advanced porous materials, smart polymers, hydrogels, nanostructured carbon, and photothermal materials, many strategies have been shown to extract freshwater and energy from atmospheric air where the tremendous amount of water and energy has previously been neglected. However, most of the techniques, so far, are designed for a single function-either for solitary water or energy harvesting.

Some recent studies have demonstrated the possibility of a two-in-one system where both water and energy can be harvested from the atmosphere. For example, the GO/PAAS composite comprises the fundamental components of both water and energy generators.[55,216] The moisture-enabled electricity generator based on an HCl/PVA gel can generate a voltage of up to 0.348 V due to moisture sorption; meanwhile, the moisture sorption of this gel can reach around 1.06 g g^{-1}.[235] A hygroscopic salt-modified corn stalk can harvest atmospheric water with a sorption capacity of 1.84 g g^{-1}, and upon coating a layer of carbon ink, it can produce an electrical voltage output of 0.6 V.[149] In most previously reported MEGs, the electricity generation was attributed to the ionic gradient built in a single moisture sorption process. In 2022, Qu's group discovered that in addition to the ionic gradient, the ion-hydration energy difference can also account for the driving force of ion movements from the less-hydrated to the more-hydrated regions, consequently generating electricity during a moisture desorption process.[263] This study has demonstrated that power generation can be integrated into a closed moisture sorption and desorption loop, which suggests concurrent atmospheric water and energy harvesting.

It is acknowledged that the hydration capacity of materials, as well as the dependence of the electrical output on materials' hydration level, is of concern when developing such a two-in-one system because it can strongly affect the water and electricity generation performance. The hydration capacity of conventional MEG materials is limited, suggesting that these materials, especially at high RH, would rapidly become water-saturated with limited water uptake and tend to produce a short-term output. Recently, Ho *et al.* reported a moisture-enabled water and electricity generator comprising an anion–cation heterostructured hydrogel (Fig. 9c).[220] Such a hydrogel heterojunction inherits a high hydration capacity and exhibits exceptional hygroscopicity for AWH. Moreover, the ionic double layer (IDL) and the built-in electric field of this heterojunction ensure a self-regulating ionic gradient for MEG, making it possible to continuously output power over a wide RH range and a stretched period. The electricity generation strongly depends on the ionic concentration in hydrogels, which can be increased by either ionization during moisture sorption or the

solution concentration during the desorption process. All these features synchronize the MEG with AWH to simultaneously generate water and energy.

3.4 Summary of mechanisms and materials' properties underpinning moisture-enabled energy generation

According to the above discussions about moisture-enabled energy generation (MEEG) technologies, it can be summarized that these technologies, including the moisture-enabled electricity generator, moisture-responsive actuator, and moisture-mediated heat battery, are based on the interactions between moisture and materials. These moisture/material interactions essentially convert the chemical potential energy difference of water molecules between a high-energy gaseous state and a low-energy absorbed state into various forms of energy, like electricity, mechanical deformation, and heat.[24,259,264] Specifically, for the moisture-electricity generator (MEG), gaseous moisture comes into contact with the MEG active materials, anchors to the functional groups of the active materials, and remains in the absorbed state, charging ions with the chemical potential energy. With an asymmetric structure, based on either the pre-determined functional group concentrations or the electrodes with different water permeabilities, the chemical potential energy of free ions is transformed into electricity through ionic diffusion. As for the moisture-responsive actuator, the released chemical potential energy is converted into mechanical energy *via* hydro-expansion of the active materials. To obtain a large deformation, an asymmetric structure is preferred for a moisture-responsive actuator, which typically assumes a bi-layered structure consisting of layers with different responses to moisture,[265,266] or a homogeneous film structure that is exposed to an environment with moisture gradients.[253,267] The moisture-mediated battery mainly exploits the heat exchange with the environment, which is accompanied by moisture sorption/desorption of the active materials. It should be noted that power generation from the evaporation-driven electricity generator stems from the energy harvested from the environment to sustain water evaporation, where moisture or steam generated by water evaporation acts as a mediator for energy generation rather than a main contributor.

As the fundamental aspect of moisture-enabled energy generation (MEEG), the moisture/material interactions can be tuned to control the performance of these energy generators. Therefore, the strategies employed to enhance the moisture/material interactions and hence, AWH are expected to also be applicable for the improvement of MEEG performance. These strategies are summarised as (1) the water affinity, (2) specific surface area, (3) porous structure, and (4) thermal/electrical conductivity. Almost all MEG materials, such as graphene oxides,[198,202–204,208–210] polymers,[205–207,211,212] cellulose fibers,[215] *etc.*, have high affinities toward water due to abundant hydrophilic surface functional groups. Hygroscopic materials, such as graphene oxides,[253] polyvinyl alcohol (PVA),[265] Nylon,[268] and moisture sorbents[259] are pivotal to the moisture-responsive actuators and the moisture-mediated heat batteries. These findings demonstrate the critical role of materials' water affinity in

12474 | *J. Mater. Chem. A*, 2023, **11**, 12456–12481

This journal is © The Royal Society of Chemistry 2023

boosting the MEEG performance. For example, introducing hygroscopic sodium polyacrylate (PAAS) into the graphene oxide (GO) framework has been proven efficacious to increase the moisture uptake of the GO/PAAS composite, which has delivered an electrical output that can last for more than 120 hours by augmenting ionic dissociation and transport.[216] Electrochemical treatment[200] and air plasma treatment[201] can be employed to create excess hydrophilic functional groups on MEG materials to elevate their water affinity efficacy and hence, their MEEG performance. As discussed, large specific surface areas signify that more atoms, functional groups, or active sites are exposed to have full interactions with moisture, while porous structures will facilitate the diffusion of water molecules within active materials to promote moisture/material interactions. This explains why most MEEG devices are made from assemblies of various nanomaterials, from quantum dots[204] to nanowires[206,256,269] to nanosheets,[5,270] where abundant active sites and hierarchical pores are synergized to provide high moisture capacity and sensitivity for energy harvesting. The efficient channels for moisture circulation endowed by the porous structure allow for a fast moisture sorption/desorption, laying the groundwork for actuators with fast response.[244,256] Also, the sorption/desorption kinetics can be accelerated by tuning the materials' thermal conductivity. MXenes ($Ti_3C_2T_x$) a type of 2D material with high thermal conductivity, have been incorporated as fillers into a polymer matrix to increase the thermal conductivity of the composite.[271] Introducing MXenes for moisture-triggered actuators can lead to a much faster response than those based on polymers.[256,265] The materials' electrical conductivity is one other key factor to be concerned with when optimizing the output power density, especially for moisture-enabled electricity generation. A certain level of electrical conductivity is required to transport charges but being too conductive will facilitate charge transfer and screen the surface change quickly, which can significantly compromise the output potential. On the other hand, high internal resistance will consume a large portion of energy and lower the output power density.[208,210] Therefore, a good trade-off between the electrical conductivity and the thickness should be considered when designing materials for MEEG.

4. Perspectives

In this review, we focus on materials and structural innovations for developing sorbents for AWH and devices for moisture-enabled energy generation. For sorbent-assisted AWH, mechanisms underlying the moisture sorption of various sorbents are discussed, followed by reviews on recent advances in designing sorbents with excellent water harvesting performance and high energy efficiency. The emerging sorbents, namely MOFs, COFs, hydrogels, and composites, as well as the smart stimuli-responsive and photothermal material incorporated sorbents, demonstrate sorbent-assisted AWH that exhibits high sorption capacity even at extremely low RH (~10–40%) with high energy efficiency. For moisture-enabled energy generation, we have discussed a variety of moisture-enabled energy conversions including electricity generation, mechanical deformation, and

thermal energy storage and management. Besides, crafting a two-in-one system for concurrent water and energy generation from moisture has been demonstrated.

Consolidated discussion on water and energy generation technologies can be rendered since both technologies are mutually based on the interaction between moisture and materials. Accordingly, enhancing the moisture/material interaction will greatly boost the performance of the moisture-enabled water and energy generators, which, from the perspective of materials design and engineering, can be achieved by improving materials' water affinity, specific surface area, porosity, and thermal/electrical conductivity. This also unravels the intrinsic link between water and energy, where advancement made on water can promote progress in energy pursuit and *vice versa*. When it comes to moisture-enabled water and energy generation, the learned lessons and wisdom can be shared between the technologies. The same material systems like GO frameworks, hydrogels, and composites have been commonly implemented for both water and energy technologies. Besides, moisture-enabled water and energy generation can be integrated into one system, for example, the two-in-one water and electricity generator, and the moisture-engaged heat batteries. These features, together with the abundance and ubiquity of moisture in air, as well as recent advances in moisture-enabled water and energy generations, illustrate that these technologies hold much promise for addressing challenges of the water-energy nexus, by offering sustainable, uninterruptable, decentralized, and off-grid access to potable water and green energy commodities.

Despite remarkable progress in recent years, it is acknowledged that studies on moisture-enabled water and energy harvesting are still in their infancy. Much of the research is still in the early stage and restrictive in scaling up. The mechanisms are not yet well-established to comprehensively explain, especially at an atomistic level, the moisture/materials interactions, the mass/energy exchange between materials and environments, as well as the water and energy generation courses. Some of these challenges and perspectives are summarized as follows.

4.1 Boosting the water and energy generation performance

High water productivity and output power density are the ultimate goals for generators, but currently, these numbers of most reported water and energy generators are still too small for practical applications, necessitating more efforts to boost their performances. Water productivity is not only dependent on the water sorption capacity of sorbents but also largely related to the moisture sorption/desorption kinetics as it will determine the number of sorption/desorption cycles and the water production within a certain time accordingly. Most of the current research tends to focus on increasing sorbents' sorption capacities or evaluating the water production on a single sorption/desorption cycle basis, with little attention paid to the sorption/desorption kinetics and the water production based on a multi-cycling mode. Therefore, the sorption/desorption kinetics of sorbents as well as the cycling performance are expected to be augmented when developing sorbents for AWH. As

This journal is © The Royal Society of Chemistry 2023

J. Mater. Chem. A, 2023, **11**, 12456–12481 | **12475**

demonstrated by recent advances in AWH sorbents, employing nanostructured materials with high specific surface area and exploring approaches to engineer and functionalize materials' surfaces will enhance the moisture/material interaction, which in turn, will improve the energy generation enabled by moisture. Thus, the progress achieved in the development of AWH sorbents, e.g., the emerging materials can work as a reference and guide for increasing the output power density.

4.2 Increasing energy conversion efficiency

For AWH, energy consumption is always of concern. Although notable progress has been made in recent years by combining smart stimuli-responsive materials and photothermal materials in sorbents, there is still a lot of room for further exploration. For example, the use of temperature-responsive polymers makes it possible to release the captured moisture and dehydrate the sorbents at a temperature as low as around 30 °C, largely reducing the consumed energy. However, most of the studies on AWH sorbents have been centered around temperature-responsive polymers, particularly PNIPAAM. Given their impressive efficacy in increasing energy efficiency, studies on a wider variety of temperature-responsive and stimuli-responsive materials are expected in the future. Currently, most photothermal materials are composited with ready-made sorbents (e.g., MOFs or hydrogels), merely acting as a light-induced heater. It is known that the thermal conductivity of carbon-based photothermal materials like CNTs and graphene oxides, are superior to that of most MOFs and hydrogels, which is desirable for high sorption/desorption kinetics. Moreover, it is possible to readily fabricate porous matrices of these carbon materials so as to engineer the properties of these materials.[55,201,272–274] Hence, this spurs the porous carbon-based photothermal materials to be directly used in a solar-driven AWH. Formulating a hybrid energy harvesting system not only achieves various moisture-enabled energy conversions, but also harnesses multiple types of low-grade energy from the environment when combined with other functional materials or structures, e.g., thermoelectric, piezoelectric, and photothermal materials. Such a synergistic design of a hybrid system will enhance the energy conversion efficiency of a moisture-enabled energy generator.

4.3 Fundamental studies

Despite the overall mechanisms available to explain moisture-enabled water and energy generation, fundamental details that can unravel the moisture/material interaction at the atomic level are not precisely grasped. For example, metal ions centered in the porous MOF structures are considered to be dominant sites for moisture capture, but recent X-ray diffraction studies on MOF-303 show that the polar organic linkers have more to do with moisture sorption.[96] The streaming potential is believed to govern the moisture-enabled electricity generation of porous carbon materials, but it is not clear how the ionic gradient mechanism plays a role in delivering power, given the fact that numerous functional groups are present on the surfaces of these carbon materials. Moreover, the electrical double layers

(EDLs) are the basis of streaming potential generation, but their structures and chemical components are theoretically predicted without sound experimental evidence. The selection and configuration of electrodes are crucial for moisture-enabled electricity generation because different electrodes may contribute differently to and even dominate electricity production, but to date, research on the effects of electrodes is scarce to further understand these fundamental issues. Hence, more fundamental studies are expected to reveal the underlying principle to guide future developments in water and energy generators.

4.4 Device-level optimization

Although this review focuses on strategies for boosting water and energy generation at the material level, future progress in device-level optimization is expected as it is required for wide and large-scale applications. Optimizing the device layout to ensure the best vapor/heat exchange between the generator and environment would promote the thermodynamics and kinetics of moisture sorption/desorption and vapor condensation, leading to enhanced water and energy productivity per volume/area. Successful integration of water and energy generation into one system would further optimize the utilization of moisture. Moreover, by effectively combining a moisture-enabled water and energy generator with other techniques like the heat battery, thermo-/pyroelectric modules, as well as seawater desalination systems, waste heat can be fully capitalized and transformed into useful energies.

Conflicts of interest

There are no conflicts to declare.

Acknowledgements

References

1 M. A. Hanjra and M. E. Qureshi, *Food Policy*, 2010, **35**, 365.
2 A. K. Biswas and C. Tortajada, *Int. J. Water Resour. Dev.*, 2019, **35**, 727.
3 S. Singh, Energy Crisis and Climate Change: Global Concerns and Their Solutions, in *Energy: Crises, Challenges and Solutions*, Wiley, 2021, p. 1.
4 M. Salehi, *Environ. Int.*, 2022, **158**, 106936.
5 M. Ye, Z. Zhang, Y. Zhao and L. Qu, *Joule*, 2018, **2**, 245.
6 S. V. Boriskina, A. Raza, T. Zhang, P. Wang, L. Zhou and J. Zhu, *MRS Bull.*, 2019, **44**, 59.
7 L. Zhu, M. Gao, C. K. N. Peh and G. W. Ho, *Nano Energy*, 2019, **57**, 507.
8 M. Gao, L. Zhu, C. K. Peh and G. W. Ho, *Energy Environ. Sci.*, 2019, **12**, 841.
9 F. Zhao, Y. Guo, X. Zhou, W. Shi and G. Yu, *Nat. Rev. Mater.*, 2020, **5**, 388.

12476 | *J. Mater. Chem. A*, 2023, **11**, 12456–12481

This journal is © The Royal Society of Chemistry 2023

10 C. Fritzmann, J. Löwenberg, T. Wintgens and T. Melin, *Desalination*, 2007, **216**, 1.

11 L. Malaeb and G. M. Ayoub, *Desalination*, 2011, **267**, 1.

12 R. V. Wahlgren, *Water Res.*, 2001, **35**, 1.

13 G. L. Stephens, J. Li, M. Wild, C. A. Clayson, N. Loeb, S. Kato, T. L'ecuyer, P. W. Stackhouse, M. Lebsock and T. Andrews, *Nat. Geosci.*, 2012, **5**, 691.

14 K. Yang, T. Pan, Q. Lei, X. Dong, Q. Cheng and Y. Han, *Environ. Sci. Technol.*, 2021, **55**, 6542.

15 Y. Tu, R. Wang, Y. Zhang and J. Wang, *Joule*, 2018, **2**, 1452.

16 X. Zhou, H. Lu, F. Zhao and G. Yu, *ACS Mater. Lett.*, 2020, **2**, 671.

17 M. Ejeian and R. Wang, *Joule*, 2021, **5**, 1678.

18 H. Lu, W. Shi, Y. Guo, W. Guan, C. Lei and G. Yu, *Adv. Mater.*, 2022, **34**, 2110079.

19 A. LaPotin, H. Kim, S. R. Rao and E. N. Wang, *Acc. Chem. Res.*, 2019, **52**, 1588.

20 W. Shi, W. Guan, C. Lei and G. Yu, *Angew. Chem., Int. Ed.*, 2022, **61**, e202211267.

21 D. Shen, W. W. Duley, P. Peng, M. Xiao, J. Feng, L. Liu, G. Zou and Y. N. Zhou, *Adv. Mater.*, 2020, **32**, 2003722.

22 Y. Huang, H. Cheng and L. Qu, *ACS Mater. Lett.*, 2021, **3**, 193.

23 X. Zhao, D. Shen, W. W. Duley, C. Tan and Y. N. Zhou, *Adv. Energy Sustainability Res.*, 2022, **3**, 2100196.

24 J. Bai, Y. Huang, H. Cheng and L. Qu, *Nanoscale*, 2019, **11**, 23083.

25 P. Guan, R. Zhu, G. Hu, R. Patterson, F. Chen, C. Liu, S. Zhang, Z. Feng, Y. Jiang and T. Wan, *Small*, 2022, **18**, 2204603.

26 Z. Zhang, X. Li, J. Yin, Y. Xu, W. Fei, M. Xue, Q. Wang, J. Zhou and W. Guo, *Nat. Nanotechnol.*, 2018, **13**, 1109.

27 L. Feng and B. Chen, *Energy Procedia*, 2016, **104**, 141.

28 A. M. Hamiche, A. B. Stambouli and S. Flazi, *Renew. Sust. Energ. Rev.*, 2016, **65**, 319.

29 T. Ding, L. Liang, K. Zhou, M. Yang and Y. Wei, *Ecol. Modell.*, 2020, **419**, 108943.

30 T. Ding and G. W. Ho, *Joule*, 2021, **5**, 1639.

31 N. Hanikel, M. S. Prévot and O. M. Yaghi, *Nat. Nanotechnol.*, 2020, **15**, 348.

32 X. Zheng, T. Ge and R. Wang, *Energy*, 2014, **74**, 280.

33 S. Namboorimadathil Backer, A. M. Ramachandran, A. A. Venugopal, A. Mohamed, A. Asok and S. Pillai, *ACS Appl. Nano Mater.*, 2020, **3**, 6827.

34 X. Wang, X. Li, G. Liu, J. Li, X. Hu, N. Xu, W. Zhao, B. Zhu and J. Zhu, *Angew. Chem.*, 2019, **131**, 12182.

35 Y. Guo, A. Al-Jubainawi and Z. Ma, *Appl. Therm. Eng.*, 2019, **149**, 1023.

36 Y. Guo, A. Al-Jubainawi and X. Peng, *Appl. Energy*, 2019, **239**, 1014.

37 Z. Xiong, Y. Dai and R. Wang, *Appl. Therm. Eng.*, 2009, **29**, 1209.

38 X. Liu, X. Yi and Y. Jiang, *Energy Convers. Manage.*, 2011, **52**, 180.

39 Y. Chen, X. Sun, C. Yan, Y. Cao and T. Mu, *J. Phys. Chem. B*, 2014, **118**, 11523.

40 H. Qi, T. Wei, W. Zhao, B. Zhu, G. Liu, P. Wang, Z. Lin, X. Wang, X. Li and X. Zhang, *Adv. Mater.*, 2019, **31**, 1903378.

41 Y. Luo, S. Shao, F. Qin, C. Tian and H. Yang, *Sol. Energy*, 2012, **86**, 2718.

42 Y. Yuan, H. Zhang, F. Yang, N. Zhang and X. Cao, *Renew. Sust. Energ. Rev.*, 2016, **54**, 761.

43 E. P. Ng and S. Mintova, *Microporous Mesoporous Mater.*, 2008, **114**, 1.

44 J. Canivet, A. Fateeva, Y. Guo, B. Coasne and D. Farrusseng, *Chem. Soc. Rev.*, 2014, **43**, 5594.

45 M. Thommes and K. A. Cychosz, *Adsorption*, 2014, **20**, 233.

46 J. Landers, G. Y. Gor and A. V. Neimark, *Colloids Surf., A*, 2013, **437**, 3.

47 D. R. Turner, M. Henry, C. Wilkinson, G. J. McIntyre, S. A. Mason, A. E. Goeta and J. W. Steed, *J. Am. Chem. Soc.*, 2005, **127**, 11063.

48 H. S. Sachar, B. S. Chava, T. H. Pial and S. Das, *Macromolecules*, 2021, **54**, 2011.

49 R. A. Jockusch, A. S. Lemoff and E. R. Williams, *J. Am. Chem. Soc.*, 2001, **123**, 12255.

50 D. Z. Vojislavljević, G. V. Janjić, D. B. Ninković, A. Kapor and S. D. Zarić, *CrystEngComm*, 2013, **15**, 2099.

51 U. Zürcher, *Eur. J. Phys.*, 2016, **38**, 015206.

52 A. Frazzica, V. Brancato, A. Caprì, C. Cannilla, L. Gordeeva and Y. Aristov, *Energy*, 2020, **208**, 118338.

53 H. Zhang, Y. Yuan, Q. Sun, X. Cao and L. Sun, *Sci. Rep.*, 2016, **6**, 1.

54 H. M. Thijs, C. R. Becer, C. Guerrero-Sanchez, D. Fournier, R. Hoogenboom and U. S. Schubert, *J. Mater. Chem.*, 2007, **17**, 4864.

55 H. Yao, P. Zhang, Y. Huang, H. Cheng, C. Li and L. Qu, *Adv. Mater.*, 2020, **32**, 1905875.

56 F. Ni, N. Qiu, P. Xiao, C. Zhang, Y. Jian, Y. Liang, W. Xie, L. Yan and T. Chen, *Angew. Chem., Int. Ed.*, 2020, **59**, 19237.

57 K. Yang, T. Pan, I. Pinnau, Z. Shi and Y. Han, *Nano Energy*, 2020, **78**, 105326.

58 F. Zhao, X. Zhou, Y. Liu, Y. Shi, Y. Dai and G. Yu, *Adv. Mater.*, 2019, **31**, 1806446.

59 M. Remko and B. M. Rode, *J. Phys. Chem. A*, 2006, **110**, 1960.

60 M. Remko, D. Fitz, R. Broer and B. M. Rode, *J. Mol. Model.*, 2011, **17**, 3117.

61 Y. I. Aristov, G. Restuccia, G. Cacciola and V. Parmon, *Appl. Therm. Eng.*, 2002, **22**, 191.

62 F. Huber, J. Berwanger, S. Polesya, S. Mankovsky, H. Ebert and F. J. Giessibl, *Science*, 2019, **366**, 235.

63 L. Gordeeva, G. Restuccia, A. Freni and Y. I. Aristov, *Fuel Process. Technol.*, 2002, **79**, 225.

64 X. Zheng, T. Ge, Y. Jiang and R. Wang, *Energy Rep.*, 2015, **51**, 24.

65 A. Entezari, T. Ge and R. Wang, *Energy*, 2018, **160**, 64.

66 D. Ovoshchnikov, I. Glaznev and Y. I. Aristov, *Kinet. Catal.*, 2011, **52**, 620.

67 Q. Yu, H. Zhao, S. Sun, H. Zhao, G. Li, M. Li and Y. Wang, *Renewable Energy*, 2019, **138**, 1087.

68 C. Y. Tso and C. Y. Chao, *Energy Rep.*, 2012, **35**, 1626.

This journal is © The Royal Society of Chemistry 2023

J. Mater. Chem. A, 2023, **11**, 12456–12481 | **12477**

69 J. Mrowiec-Białoń, A. B. Jarzebski, A. I. Lachowski, J. J. Malinowski and Y. I. Aristov, *Chem. Mater.*, 1997, **9**, 2486.

70 X. Bu, L. Wang and Y. Huang, *Adsorption*, 2013, **19**, 929.

71 K. M. Sukhyy, E. A. Belyanovskaya, Y. N. Kozlov, E. V. Kolomiyets and M. P. Sukhyy, *Appl. Therm. Eng.*, 2014, **64**, 408.

72 X. Zheng, T. Ge, R. Wang and L. Hu, *Chem. Eng. Sci.*, 2014, **120**, 1.

73 M. Ignat, P. Samoila, C. Cojocaru, G. Soreanu, I. Cretescu and V. Harabagiu, *Appl. Surf. Sci.*, 2019, **487**, 1189.

74 R. Liu, T. Gong, K. Zhang and C. Lee, *Sci. Rep.*, 2017, **7**, 1.

75 F. Miksik, T. Miyazaki, K. Thu, J. Miyawaki, K. Nakabayashi, A. T. Wijayanta and F. Rahmawati, *Energy Rep*, 2021, **7**, 5871.

76 X. Wei, W. Wang, J. Xiao, L. Zhang, H. Chen and J. Ding, *Chem. Eng. J.*, 2013, **228**, 1133.

77 C. Wang, B. Yang, X. Ji, R. Zhang and H. Wu, *Energy*, 2022, **251**, 123874.

78 J. Chao, J. Xu, T. Yan, P. Wang, X. Huo, R. Wang and T. Li, *Energy*, 2022, **240**, 122797.

79 O. M. Yaghi, M. O'Keeffe, N. W. Ockwig, H. K. Chae, M. Eddaoudi and J. Kim, *Nature*, 2003, **423**, 705.

80 S. R. Batten, N. R. Champness, X. M. Chen, J. Garcia-Martinez, S. Kitagawa, L. Öhrström, M. O'Keeffe, M. P. Suh and J. Reedijk, *Pure Appl. Chem.*, 2013, **85**, 1715.

81 S. Wang, W. Yao, J. Lin, Z. Ding and X. Wang, *Angew. Chem.*, 2014, **126**, 1052.

82 S. Wang and X. Wang, *Small*, 2015, **11**, 3097.

83 R. Freund, O. Zaremba, G. Arnauts, R. Ameloot, G. Skorupskii, M. Dincă, A. Bavykina, J. Gascon, A. Ejsmont and J. Goscianska, *Angew. Chem., Int. Ed.*, 2021, **60**, 23975.

84 S. M. T. Abtab, D. Alezi, P. M. Bhatt, A. Shkurenko, Y. Belmabkhout, H. Aggarwal, Ł. J. Weseliński, N. Alsadun, U. Samin and M. N. Hedhili, *Chem*, 2018, **4**, 94.

85 F. Fathieh, M. J. Kalmutzki, E. A. Kapustin, P. J. Waller, J. Yang and O. M. Yaghi, *Sci. Adv.*, 2018, **4**, eaat3198.

86 M. J. Kalmutzki, C. S. Diercks and O. M. Yaghi, *Adv. Mater.*, 2018, **30**, 1704304.

87 P. D. Dietzel, R. E. Johnsen, R. Blom and H. Fjellvåg, *Eur. J. Chem.*, 2008, **14**, 2389.

88 P. Küsgens, M. Rose, I. Senkovska, H. Fröde, A. Henschel, S. Siegle and S. Kaskel, *Microporous Mesoporous Mater.*, 2009, **120**, 325.

89 G. E. Cmarik, M. Kim, S. M. Cohen and K. S. Walton, *Langmuir*, 2012, **28**, 15606.

90 J. Ehrenmann, S. K. Henninger and C. Janiak, *Eur. J. Inorg. Chem.*, 2011, **2011**, 471.

91 H. Furukawa, F. Gandara, Y. B. Zhang, J. Jiang, W. L. Queen, M. R. Hudson and O. M. Yaghi, *J. Am. Chem. Soc.*, 2014, **136**, 4369.

92 H. Kim, S. R. Rao, E. A. Kapustin, L. Zhao, S. Yang, O. M. Yaghi and E. N. Wang, *Nat. Commun.*, 2018, **9**, 1.

93 H. Kim, S. Yang, S. R. Rao, S. Narayanan, E. A. Kapustin, H. Furukawa, A. S. Umans, O. M. Yaghi and E. N. Wang, *Science*, 2017, **356**, 430.

94 A. J. Rieth, S. Yang, E. N. Wang and M. Dincă, *ACS Cent. Sci.*, 2017, **3**, 668.

95 N. Hanikel, M. S. Prévot, F. Fathieh, E. A. Kapustin, H. Lyu, H. Wang, N. J. Diercks, T. G. Glover and O. M. Yaghi, *ACS Cent. Sci.*, 2019, **5**, 1699.

96 N. Hanikel, X. Pei, S. Chheda, H. Lyu, W. Jeong, J. Sauer, L. Gagliardi and O. M. Yaghi, *Science*, 2021, **374**, 454.

97 Y. Song, N. Xu, G. Liu, H. Qi, W. Zhao, B. Zhu, L. Zhou and J. Zhu, *Nat. Nanotechnol.*, 2022, **17**, 857.

98 J. J. Low, A. I. Benin, P. Jakubczak, J. F. Abrahamian, S. A. Faheem and R. R. Willis, *J. Am. Chem. Soc.*, 2009, **131**, 15834.

99 T. Pan, K. Yang and Y. Han, *Chem. Res. Chin. Univ.*, 2020, **36**, 33.

100 H. J. Choi, M. Dincă, A. Dailly and J. R. Long, *Energy Environ. Sci.*, 2010, **3**, 117.

101 K. S. Park, Z. Ni, A. P. Côté, J. Y. Choi, R. Huang, F. J. Uribe-Romo, H. K. Chae, M. O'Keeffe and O. M. Yaghi, *Proc. Natl. Acad. Sci. U.S.A.*, 2006, **103**, 10186.

102 H. Jasuja, Y.-g. Huang and K. S. Walton, *Langmuir*, 2012, **28**, 16874.

103 L. Bellarosa, J. J. Gutiérrez-Sevillano, S. Calero and N. López, *Phys. Chem. Chem. Phys.*, 2013, **15**, 17696.

104 I. J. Kang, N. A. Khan, E. Haque and S. H. Jhung, *Eur. J. Chem.*, 2011, **17**, 6437.

105 Y. Z. Zhang, T. He, X. J. Kong, X. L. Lv, X. Q. Wu and J. R. Li, *ACS Appl. Mater. Interfaces*, 2018, **10**, 27868.

106 H. Reinsch, M. A. van der Veen, B. Gil, B. Marszalek, T. Verbiest, D. De Vos and N. Stock, *Chem. Mater.*, 2013, **25**, 17.

107 M. Nemiwal, V. Sharma and D. Kumar, *Mini-Rev. Org. Chem.*, 2021, **18**, 1026.

108 C. S. Diercks and O. M. Yaghi, *Science*, 2017, **355**, eaal1585.

109 S. Y. Ding and W. Wang, *Chem. Soc. Rev.*, 2013, **42**, 548.

110 X. Feng, X. Ding and D. Jiang, *Chem. Soc. Rev.*, 2012, **41**, 6010.

111 A. Nagai, Z. Guo, X. Feng, S. Jin, X. Chen, X. Ding and D. Jiang, *Nat. Commun.*, 2011, **2**, 1.

112 A. P. Cote, A. I. Benin, N. W. Ockwig, M. O'Keeffe, A. J. Matzger and O. M. Yaghi, *Science*, 2005, **310**, 1166.

113 Y. Byun, S. H. Je, S. N. Talapaneni and A. Coskun, *Eur. J. Chem.*, 2019, **25**, 10262.

114 B. P. Biswal, S. Kandambeth, S. Chandra, D. B. Shinde, S. Bera, S. Karak, B. Garai, U. K. Kharul and R. Banerjee, *J. Mater. Chem. A*, 2015, **3**, 23664.

115 H. L. Nguyen, N. Hanikel, S. J. Lyle, C. Zhu, D. M. Proserpio and O. M. Yaghi, *J. Am. Chem. Soc.*, 2020, **142**, 2218.

116 A. S. Hoffman, *Adv. Drug Deliv. Rev.*, 2012, **64**, 18.

117 F. Deng, Z. Chen, C. Wang, C. Xiang, P. Poredoš and R. Wang, *Adv. Sci.*, 2022, **9**, 2204724.

118 M. Wu, R. Li, Y. Shi, M. Altunkaya, S. Aleid, C. Zhang, W. Wang and P. Wang, *Mater. Horiz.*, 2021, **8**, 1518.

119 D. K. Nandakumar, Y. Zhang, S. K. Ravi, N. Guo, C. Zhang and S. C. Tan, *Adv. Mater.*, 2019, **31**, 1806730.

120 D. K. Nandakumar, S. K. Ravi, Y. Zhang, N. Guo, C. Zhang and S. C. Tan, *Energy Environ. Sci.*, 2018, **11**, 2179.

12478 | *J. Mater. Chem. A*, 2023, **11**, 12456–12481

This journal is © The Royal Society of Chemistry 2023

121 J. Xu, T. Li, J. Chao, S. Wu, T. Yan, W. Li, B. Cao and R. Wang, *Angew. Chem., Int. Ed.*, 2020, **59**, 5202.

122 S. Aleid, M. Wu, R. Li, W. Wang, C. Zhang, L. Zhang and P. Wang, *ACS Mater. Lett.*, 2022, **4**, 511.

123 C. D. Díaz-Marín, L. Zhang, Z. Lu, M. Alshrah, J. C. Grossman and E. N. Wang, *Nano Lett.*, 2022, **22**, 1100.

124 Y. Guo, Z. Fang and G. Yu, *Polym. Int.*, 2021, **70**, 1425.

125 F. Zhao, J. Bae, X. Zhou, Y. Guo and G. Yu, *Adv. Mater.*, 2018, **30**, 1801796.

126 H. Zhao, Z. Zhang, H. Hou and J. Zhang, *J. Solid State Chem.*, 2021, **301**, 122304.

127 H. Zhao, M. Lei, T. Liu, T. Huang and M. Zhang, *Inorg. Chim. Acta*, 2020, **511**, 119842.

128 Y. Sun, A. Spieß, C. Jansen, A. Nuhnen, S. Gökpinar, R. Wiedey, S. J. Ernst and C. Janiak, *J. Mater. Chem. A*, 2020, **8**, 13364.

129 R. Li, Y. Shi, M. Alsaedi, M. Wu, L. Shi and P. Wang, *Environ. Sci. Technol.*, 2018, **52**, 11367.

130 P. A. Kallenberger and M. Fröba, *Chem. Commun.*, 2018, **1**, 1.

131 A. Entezari, M. Ejeian and R. Wang, *ACS Mater. Lett.*, 2020, **2**, 471.

132 C. Lei, Y. Guo, W. Guan, H. Lu, W. Shi and G. Yu, *Angew. Chem., Int. Ed.*, 2022, **61**, e202200271.

133 K. Matsumoto, N. Sakikawa and T. Miyata, *Nat. Commun.*, 2018, **9**, 1.

134 H. Shan, Q. Pan, C. Xiang, P. Poredoš, Q. Ma, Z. Ye, G. Hou and R. Wang, *Cell Rep. Phys. Sci.*, 2021, **2**, 100664.

135 M. Ejeian, A. Entezari and R. Wang, *Appl. Therm. Eng.*, 2020, **176**, 115396.

136 A. Entezari, M. Ejeian and R. Wang, *Mater. Today Energy*, 2019, **13**, 362.

137 R. Li, Y. Shi, M. Wu, S. Hong and P. Wang, *Nano Energy*, 2020, **67**, 104255.

138 P. Tao, G. Ni, C. Song, W. Shang, J. Wu, J. Zhu, G. Chen and T. Deng, *Nat. Energy*, 2018, **3**, 1031.

139 R. Li, Y. Shi, L. Shi, M. Alsaedi and P. Wang, *Environ. Sci. Technol.*, 2018, **52**, 5398.

140 T. Lyu, Z. Wang, R. Liu, K. Chen, H. Liu and Y. Tian, *ACS Appl. Mater. Interfaces*, 2022, **14**, 32433.

141 X. Zhou, F. Zhao, Y. Guo, B. Rosenberger and G. Yu, *Sci. Adv.*, 2019, **5**, eaaw5484.

142 G. Yilmaz, F. Meng, W. Lu, J. Abed, C. Peh, M. Gao, E. Sargent and G. Ho, *Sci. Adv.*, 2020, **6**, eabc8605.

143 A. Mulchandani, S. Malinda, J. Edberg and P. Westerhoff, *Environ. Sci. Nano*, 2020, **7**, 2584.

144 M. Wang, T. Sun, D. Wan, M. Dai, S. Ling, J. Wang, Y. Liu, Y. Fang, S. Xu and J. Yeo, *Nano Energy*, 2021, **80**, 105569.

145 X. Wang, D. Yang, M. Zhang, Q. Hu, K. Gao, J. Zhou and Z. Z. Yu, *ACS Appl. Mater. Interfaces*, 2022, **14**, 33881.

146 H. Park, I. Haechler, G. Schnoering, M. D. Ponte, T. M. Schutzius and D. Poulikakos, *ACS Appl. Mater. Interfaces*, 2022, **14**, 2237.

147 F. Deng, C. Wang, C. Xiang and R. Wang, *Nano Energy*, 2021, **90**, 106642.

148 Y. Zhang, L. Wu, X. Wang, J. Yu and B. Ding, *Nat. Commun.*, 2020, **11**, 1.

149 F. Gong, H. Li, Q. Zhou, M. Wang, W. Wang, Y. Lv, R. Xiao and D. V. Papavassiliou, *Nano Energy*, 2020, **74**, 104922.

150 K. Lu, C. Liu, J. Liu, Y. He, X. Tian, Z. Liu, Y. Cao, Y. Shen, W. Huang and K. Zhang, *ACS Appl. Mater. Interfaces*, 2022, **14**, 33032.

151 F. Ni, P. Xiao, N. Qiu, C. Zhang, Y. Liang, J. Gu, J. Xia, Z. Zeng, L. Wang and Q. Xue, *Nano Energy*, 2020, **68**, 104311.

152 F. Liu and M. W. Urban, *Prog. Polym. Sci.*, 2010, **35**, 3.

153 M. A. C. Stuart, W. T. Huck, J. Genzer, M. Müller, C. Ober, M. Stamm, G. B. Sukhorukov, I. Szleifer, V. V. Tsukruk and M. Urban, *Nat. Mater.*, 2010, **9**, 101.

154 M. Wei, Y. Gao, X. Li and M. J. Serpe, *Polym. Chem.*, 2017, **8**, 127.

155 P. Bawa, V. Pillay, Y. E. Choonara and L. C. Du Toit, *Biomed. Mater.*, 2009, **4**, 022001.

156 E. Cabane, X. Zhang, K. Langowska, C. G. Palivan and W. Meier, *Biointerphases*, 2012, **7**, 9.

157 Y. L. Colson and M. W. Grinstaff, *Adv. Mater.*, 2012, **24**, 3878.

158 L. Zhai, *Chem. Soc. Rev.*, 2013, **42**, 7148.

159 P. F. Cao, J. D. Mangadlao and R. C. Advincula, *Polym. Rev.*, 2015, **55**, 706.

160 Y. J. Kim and Y. T. Matsunaga, *J. Mater. Chem. B*, 2017, **5**, 4307.

161 A. Karmakar, P. G. Mileo, I. Bok, S. B. Peh, J. Zhang, H. Yuan, G. Maurin and D. Zhao, *Angew. Chem., Int. Ed.*, 2020, **59**, 11159.

162 X. Liu, Y. Li, J. Hu, J. Jiao and J. Li, *RSC Adv.*, 2014, **4**, 63691.

163 N. Thakur, A. Sargur Ranganath, K. Sopiha and A. Baji, *ACS Appl. Mater. Interfaces*, 2017, **9**, 29224.

164 H. Okuzaki, K. Kobayashi and H. Yan, *Synth. Met.*, 2009, **159**, 2273.

165 N. Thakur, A. Baji and A. S. Ranganath, *Appl. Surf. Sci.*, 2018, **433**, 1018.

166 C. Morris, B. Szczupak, A. S. Klymchenko and A. G. Ryder, *Macromolecules*, 2010, **43**, 9488.

167 V. A. Ganesh, A. S. Ranganath, R. Sridhar, H. K. Raut, S. Jayaraman, R. Sahay, S. Ramakrishna and A. Baji, *Macromol. Rapid Commun.*, 2015, **36**, 1368.

168 A. S. Ranganath, V. A. Ganesh, K. Sopiha, R. Sahay and A. Baji, *RSC Adv.*, 2017, **7**, 19982.

169 X. André, M. Zhang and A. H. Müller, *Macromol. Rapid Commun.*, 2005, **26**, 558.

170 J. Ramos, A. Imaz and J. Forcada, *Polym. Chem.*, 2012, **3**, 852.

171 N. A. Cortez-Lemus and A. Licea-Claverie, *Prog. Polym. Sci.*, 2016, **53**, 1.

172 S. Kim, Y. Liang, S. Kang and H. Choi, *Chem. Eng. J.*, 2021, **425**, 131601.

173 K. F. Arndt, T. Schmidt and R. Reichelt, *Polymer*, 2001, **42**, 6785.

174 J. S. Park, Y. Akiyama, F. M. Winnik and K. Kataoka, *Macromolecules*, 2004, **37**, 6786.

175 K. N. Plunkett, X. Zhu, J. S. Moore and D. E. Leckband, *Langmuir*, 2006, **22**, 4259.

This journal is © The Royal Society of Chemistry 2023

J. Mater. Chem. A, 2023, **11**, 12456–12481 | **12479**

176 R. Hoogenboom, H. M. Thijs, M. J. Jochems, B. M. van Lankvelt, M. W. Fijten and U. S. Schubert, *Chem. Commun.*, 2008, 5758.

177 Y. Katsumoto and N. Kubosaki, *Macromolecules*, 2008, **41**, 5955.

178 P. J. Roth, F. D. Jochum, F. R. Forst, R. Zentel and P. Theato, *Macromolecules*, 2010, **43**, 4638.

179 S. Furyk, Y. Zhang, D. Ortiz-Acosta, P. S. Cremer and D. E. Bergbreiter, *J. Polym. Sci., Part A: Polym. Chem.*, 2006, **44**, 1492.

180 L. Yu and J. Ding, *Chem. Soc. Rev.*, 2008, **37**, 1473.

181 S. Huber and R. Jordan, *Colloid Polym. Sci.*, 2008, **286**, 395.

182 F. Meersman, J. Wang, Y. Wu and K. Heremans, *Macromolecules*, 2005, **38**, 8923.

183 R. Cheng, F. Meng, C. Deng, H. A. Klok and Z. Zhong, *Biomaterials*, 2013, **34**, 3647.

184 P. Schattling, F. D. Jochum and P. Theato, *Polym. Chem.*, 2014, **5**, 25.

185 S. Guragain, B. P. Bastakoti, V. Malgras, K. Nakashima and Y. Yamauchi, *Eur. J. Chem.*, 2015, **21**, 13164.

186 Y. Tao, Q. Wu, C. Huang, D. Zhu and H. Li, *Chem. Eng. J.*, 2023, **451**, 138547.

187 Q. Li, Y. Ying, Y. Tao and H. Li, *Ind. Eng. Chem. Res.*, 2022, **61**, 1344.

188 Y. Tao, Q. Li, Q. Wu and H. Li, *Mater. Horiz.*, 2021, **8**, 1439.

189 A. LaPotin, Y. Zhong, L. Zhang, L. Zhao, A. Leroy, H. Kim, S. R. Rao and E. N. Wang, *Joule*, 2021, **5**, 166.

190 M. Kumar and A. Yadav, *J. Renew. Sustain. Energy*, 2015, **7**, 033122.

191 M. Kumar and A. Yadav, *Desalination*, 2015, **367**, 216.

192 G. E. William, M. Mohamed and M. Fatouh, *Energy*, 2015, **90**, 1707.

193 M. Elashmawy, *J. Clean. Prod.*, 2020, **249**, 119322.

194 M. Elashmawy and F. Alshammari, *J. Clean. Prod.*, 2020, **256**, 120329.

195 Q. Wu, W. Su, Q. Li, Y. Tao and H. Li, *ACS Appl. Mater. Interfaces*, 2021, **13**, 38906.

196 G. Liu, T. Chen, J. Xu and K. Wang, *J. Mater. Chem. A*, 2018, **6**, 18357.

197 Y. Xu, P. Chen and H. Peng, *Eur. J. Chem.*, 2018, **24**, 6287.

198 Y. Huang, H. Cheng, C. Yang, P. Zhang, Q. Liao, H. Yao, G. Shi and L. Qu, *Nat. Commun.*, 2018, **9**, 1.

199 H. Wang, Y. Sun, T. He, Y. Huang, H. Cheng, C. Li, D. Xie, P. Yang, Y. Zhang and L. Qu, *Nat. Nanotechnol.*, 2021, **16**, 811.

200 F. Zhao, Y. Liang, H. Cheng, L. Jiang and L. Qu, *Energy Environ. Sci.*, 2016, **9**, 912.

201 K. Liu, P. Yang, S. Li, J. Li, T. Ding, G. Xue, Q. Chen, G. Feng and J. Zhou, *Angew. Chem., Int. Ed.*, 2016, **55**, 8003.

202 Y. Liang, F. Zhao, Z. Cheng, Q. Zhou, H. Shao, L. Jiang and L. Qu, *Nano Energy*, 2017, **32**, 329.

203 S. Lee, H. Jang, H. Lee, D. Yoon and S. Jeon, *ACS Appl. Mater. Interfaces*, 2019, **11**, 26970.

204 Y. Huang, H. Cheng, G. Shi and L. Qu, *ACS Appl. Mater. Interfaces*, 2017, **9**, 38170.

205 S. Lee, J. Eun and S. Jeon, *Nano Energy*, 2020, **68**, 104364.

206 X. Nie, B. Ji, N. Chen, Y. Liang, Q. Han and L. Qu, *Nano Energy*, 2018, **46**, 297.

207 N. Chen, Q. Liu, C. Liu, G. Zhang, J. Jing, C. Shao, Y. Han and L. Qu, *Nano Energy*, 2019, **65**, 104047.

208 H. Cheng, Y. Huang, F. Zhao, C. Yang, P. Zhang, L. Jiang, G. Shi and L. Qu, *Energy Environ. Sci.*, 2018, **11**, 2839.

209 H. Cheng, Y. Huang, L. Qu, Q. Cheng, G. Shi and L. Jiang, *Nano Energy*, 2018, **45**, 37.

210 F. Zhao, H. Cheng, Z. Zhang, L. Jiang and L. Qu, *Adv. Mater.*, 2015, **27**, 4351.

211 J. Xue, F. Zhao, C. Hu, Y. Zhao, H. Luo, L. Dai and L. Qu, *Adv. Funct. Mater.*, 2016, **26**, 8784.

212 H. Wang, H. Cheng, Y. Huang, C. Yang, D. Wang, C. Li and L. Qu, *Nano Energy*, 2020, **67**, 104238.

213 Y. Liang, F. Zhao, Z. Cheng, Y. Deng, Y. Xiao, H. Cheng, P. Zhang, Y. Huang, H. Shao and L. Qu, *Energy Environ. Sci.*, 2018, **11**, 1730.

214 T. Xu, X. Ding, Y. Huang, C. Shao, L. Song, X. Gao, Z. Zhang and L. Qu, *Energy Environ. Sci.*, 2019, **12**, 972.

215 X. Liu, H. Gao, J. E. Ward, X. Liu, B. Yin, T. Fu, J. Chen, D. R. Lovley and J. Yao, *Nature*, 2020, **578**, 550.

216 Y. Huang, H. Cheng, C. Yang, H. Yao, C. Li and L. Qu, *Energy Environ. Sci.*, 2019, **12**, 1848.

217 G. Ren, Z. Wang, B. Zhang, X. Liu, J. Ye, Q. Hu and S. Zhou, *Nano Energy*, 2021, **89**, 106361.

218 W. Yang, X. Li, X. Han, W. Zhang, Z. Wang, X. Ma, M. Li and C. Li, *Nano Energy*, 2020, **71**, 104610.

219 W. Yang, L. Lv, X. Li, X. Han, M. Li and C. Li, *ACS Nano*, 2020, **14**, 10600.

220 W. Lu, T. Ding, X. Wang, C. Zhang, T. Li, K. Zeng and G. W. Ho, *Nano Energy*, 2022, **104**, 107892.

221 D. C. Grahame, *Chem. Rev.*, 1947, **41**, 441.

222 R. Parsons, *Chem. Rev.*, 1990, **90**, 813.

223 J. Maier, *Solid State Ionics*, 2002, **154**, 291.

224 T. Ding, K. Liu, J. Li, G. Xue, Q. Chen, L. Huang, B. Hu and J. Zhou, *Adv. Funct. Mater.*, 2017, **27**, 1700551.

225 G. Xue, Y. Xu, T. Ding, J. Li, J. Yin, W. Fei, Y. Cao, J. Yu, L. Yuan and L. Gong, *Nat. Nanotechnol.*, 2017, **12**, 317.

226 J. Li, K. Liu, T. Ding, P. Yang, J. Duan and J. Zhou, *Nano Energy*, 2019, **58**, 797.

227 Y. Qin, Y. Wang, X. Sun, Y. Li, H. Xu, Y. Tan, Y. Li, T. Song and B. Sun, *Angew. Chem.*, 2020, **132**, 10706.

228 X. Zhou, W. Zhang, C. Zhang, Y. Tan, J. Guo, Z. Sun and X. Deng, *ACS Appl. Mater. Interfaces*, 2020, **12**, 11232.

229 D. Shen, M. Xiao, G. Zou, L. Liu, W. W. Duley and Y. N. Zhou, *Adv. Mater.*, 2018, **30**, 1705925.

230 B. Ji, N. Chen, C. Shao, Q. Liu, J. Gao, T. Xu, H. Cheng and L. Qu, *J. Mater. Chem. A*, 2019, **7**, 6766.

231 J. Chi, C. Liu, L. Che, D. Li, K. Fan, Q. Li, W. Yang, L. Dong, G. Wang and Z. L. Wang, *Adv. Sci.*, 2022, **9**, 2201586.

232 L. Li, S. Feng, Y. Bai, X. Yang, M. Liu, M. Hao, S. Wang, Y. Wu, F. Sun and Z. Liu, *Nat. Commun.*, 2022, **13**, 1.

233 Q. Hu, Y. Ma, G. Ren, B. Zhang and S. Zhou, *Sci. Adv.*, 2022, **8**, eabm8047.

234 S. G. Yoon, Y. Yang, J. Yoo, H. Jin, W. H. Lee, J. Park and Y. S. Kim, *ACS Appl. Electron. Mater.*, 2019, **1**, 1746.

235 Z. Luo, C. Liu and S. Fan, *Nano Energy*, 2019, **60**, 371.

12480 | *J. Mater. Chem. A*, 2023, **11**, 12456–12481

This journal is © The Royal Society of Chemistry 2023

236 J. Bae, T. G. Yun, B. L. Suh, J. Kim and I. D. Kim, *Energy Environ. Sci.*, 2020, **13**, 527.

237 I. Agnarsson, A. Dhinojwala, V. Sahni and T. A. Blackledge, *J. Exp. Biol.*, 2009, **212**, 1990.

238 X. Chen, L. Mahadevan, A. Driks and O. Sahin, *Nat. Nanotechnol.*, 2014, **9**, 137.

239 M. Rüggeberg and I. Burgert, *PLoS One*, 2015, **10**, e0120718.

240 E. Reyssat and L. Mahadevan, *Europhys. Lett.*, 2011, **93**, 54001.

241 Y. Park and X. Chen, *J. Mater. Chem. A*, 2020, **8**, 15227.

242 M. Ma, L. Guo, D. G. Anderson and R. Langer, *Science*, 2013, **339**, 186.

243 H. Arazoe, D. Miyajima, K. Akaike, F. Araoka, E. Sato, T. Hikima, M. Kawamoto and T. Aida, *Nat. Mater.*, 2016, **15**, 1084.

244 M. Yang, S. Q. Wang, Z. Liu, Y. Chen, M. J. Zaworotko, P. Cheng, J. G. Ma and Z. Zhang, *J. Am. Chem. Soc.*, 2021, **143**, 7732.

245 C. Lv, H. Xia, Q. Shi, G. Wang, Y. S. Wang, Q. D. Chen, Y. L. Zhang, L. Q. Liu and H. B. Sun, *Adv. Mater. Interfaces*, 2017, **4**, 1601002.

246 B. Shin, J. Ha, M. Lee, K. Park, G. H. Park, T. H. Choi, K. J. Cho and H. Y. Kim, *Sci. Robot.*, 2018, **3**, eaar2629.

247 W. Wang, C. Xiang, Q. Liu, M. Li, W. Zhong, K. Yan and D. Wang, *J. Mater. Chem. A*, 2018, **6**, 22599.

248 L. T. de Haan, J. M. Verjans, D. J. Broer, C. W. Bastiaansen and A. P. Schenning, *J. Am. Chem. Soc.*, 2014, **136**, 10585.

249 H. Cheng, Y. Hu, F. Zhao, Z. Dong, Y. Wang, N. Chen, Z. Zhang and L. Qu, *Adv. Mater.*, 2014, **26**, 2909.

250 S. He, P. Chen, L. Qiu, B. Wang, X. Sun, Y. Xu and H. Peng, *Angew. Chem., Int. Ed.*, 2015, **54**, 14880.

251 H. Cheng, J. Liu, Y. Zhao, C. Hu, Z. Zhang, N. Chen, L. Jiang and L. Qu, *Angew. Chem., Int. Ed.*, 2013, **52**, 10482.

252 X. Gu, Q. Fan, F. Yang, L. Cai, N. Zhang, W. Zhou, W. Zhou and S. Xie, *Nanoscale*, 2016, **8**, 17881.

253 Y. Ge, R. Cao, S. Ye, Z. Chen, Z. Zhu, Y. Tu, D. Ge and X. Yang, *Chem. Commun.*, 2018, **54**, 3126.

254 X. Chen, D. Goodnight, Z. Gao, A. H. Cavusoglu, N. Sabharwal, M. DeLay, A. Driks and O. Sahin, *Nat. Commun.*, 2015, **6**, 1.

255 J. He, P. Xiao, J. Zhang, Z. Liu, W. Wang, L. Qu, Q. Ouyang, X. Wang, Y. Chen and T. Chen, *Adv. Mater. Interfaces*, 2016, **3**, 1600169.

256 L. Yang, J. Cui, L. Zhang, X. Xu, X. Chen and D. Sun, *Adv. Funct. Mater.*, 2021, **31**, 2101378.

257 K. Yang, Y. Shi, M. Wu, W. Wang, Y. Jin, R. Li, M. W. Shahzad, K. C. Ng and P. Wang, *J. Mater. Chem. A*, 2020, **8**, 1887.

258 Y. Zhang and R. Wang, *Energy Storage Mater.*, 2020, **27**, 352.

259 N. Yu, R. Wang and L. Wang, *Prog. Energy Combust. Sci.*, 2013, **39**, 489.

260 L. Zhu, T. Ding, M. Gao, C. K. N. Peh and G. W. Ho, *Adv. Energy Mater.*, 2019, **9**, 1900250.

261 T. Ding, L. Zhu, X. Q. Wang, K. H. Chan, X. Lu, Y. Cheng and G. W. Ho, *Adv. Energy Mater.*, 2018, **8**, 1802397.

262 T. Ding, Y. Zhou, W. L. Ong and G. W. Ho, *Mater. Today*, 2021, **42**, 178.

263 H. Wang, T. He, X. Hao, Y. Huang, H. Yao, F. Liu, H. Cheng and L. Qu, *Nat. Commun.*, 2022, **13**, 1.

264 T. Xu, Q. Han, Z. Cheng, J. Zhang and L. Qu, *Small Methods*, 2018, **2**, 1800108.

265 S. Xing, P. Wang, S. Liu, Y. Xu, R. Zheng, Z. Deng, Z. Peng, J. Li, Y. Wu and L. Liu, *Compos. Sci. Technol.*, 2020, **193**, 108133.

266 J. Wang, Y. Liu, Z. Cheng, Z. Xie, L. Yin, W. Wang, Y. Song, H. Zhang, Y. Wang and Z. Fan, *Angew. Chem., Int. Ed.*, 2020, **59**, 14029.

267 Z. Zhao, Y. Hwang, Y. Yang, T. Fan, J. Song, S. Suresh and N.-J. Cho, *Proc. Natl. Acad. Sci. U.S.A.*, 2020, **117**, 8711.

268 X. Li, B. Ma, J. Dai, C. Sui, D. Pande, D. R. Smith, L. C. Brinson and P. C. Hsu, *Sci. Adv.*, 2021, **7**, eabj7906.

269 X. Liu, T. Fu, J. Ward, H. Gao, B. Yin, T. Woodard, D. R. Lovley and J. Yao, *Adv. Electron. Mater.*, 2020, **6**, 2000721.

270 Y. Q. Liu, Z. D. Chen, D. D. Han, J. W. Mao, J. N. Ma, Y. L. Zhang and H. B. Sun, *Adv. Sci.*, 2021, **8**, 2002464.

271 L. Chen, Y. Cao, X. Zhang, X. Guo, P. Song, K. Chen and J. Lin, *J. Mater. Sci.*, 2020, **55**, 16533.

272 J. S. Yu, S. Kang, S. B. Yoon and G. Chai, *J. Am. Chem. Soc.*, 2002, **124**, 9382.

273 J. W. Burress, S. Gadipelli, J. Ford, J. M. Simmons, W. Zhou and T. Yildirim, *Angew. Chem., Int. Ed.*, 2010, **49**, 8902.

274 S. Dutta, A. Bhaumik and K. C. W. Wu, *Energy Environ. Sci.*, 2014, **7**, 3574.

This journal is © The Royal Society of Chemistry 2023

J. Mater. Chem. A, 2023, **11**, 12456–12481 | **12481**